＜特別寄稿＞

日本肝臓学会コンセンサス神戸2009：NASHの診断と治療

岡上　武[1]　西原　利治[2]*　小野　正文[2]　角田　圭雄[3]　橋本　悦子[4]
田村　信司[5]　山田剛太郎[6]　河田　純男[7]　工藤　正俊[8]

索引用語：　酸化ストレス　インスリン抵抗性　メタボリックシンドローム
肝硬変　肝細胞癌

はじめに

1980年Mayo Clinicの病理学者であったLudwigはアルコール性肝炎に類似する肝組織所見を呈した飲酒歴に乏しい症例について，既知の疾患を可能な限り除外し得た20症例を呈示し，非アルコール性脂肪肝炎(nonalcoholic steatohepatitis: NASH)として報告した[1]（Table 1）．本症は単なる糖尿病の合併症ではなく，主として肥満などの生活習慣病を誘因として発症する慢性進行性肝疾患で，肝硬変から肝不全や肝細胞癌にまで進展する生活習慣病の肝臓における表現形と認識されている．しかし，肥満を誘因とするNASH以外にも消化管手術後，睡眠時無呼吸症候群，神経性食思不振症やある種の薬剤服用などでも発症する症例が存在するため，誘因により各々を区別し，診断名に付記することが提案された（Table 1）．Schaffnerらも1986年に，飲酒量がエタノール換算で20 g/日以下にもかかわらずアルコール性肝障害に類似した組織像を示す疾患について，既知の疾患を可能な限り除外した症例を非アルコール性脂肪肝疾患（nonalcoholic fatty liver disease: NAFLD）として報告した[2]．その後，1990年にはWanlessらが同様の組織学的変化を示す剖検例を多数解析して，fatty liver hepatitisとして報告した[3]．病理学的視点に立ったこれらの論文を通じて，肝硬変や肝細胞癌の温床となるNASHの存在が明確となり，1998年のNIH ConferenceでNASHという病理学的に診断に基づく新しい疾患概念が確立された．

本邦で最初にNASHが主題として取り上げられたのは2001年の日本肝臓学会西部会であり，2004年には欧米およびアジアの専門家が一同に会して日本肝臓学会Single Topic Conferenceが開かれた．その後，2006年に日本肝臓学会の編集によるNASH・NAFLDの診療ガイド[4]が上梓されるや，国内，国外でNASH/NAFLDに関する多くの報告[5]がなされるようになった．NASHがこのように日常診療で広く取り扱われるようになるにつれ，診療の根拠となる共通認識形成やエビデンスに基づく推奨事項の文書化を求める声が高まった．しかし，わが国ではNASHの臨床・研究が本格的に幅広く行われだして10年程しか経過しておらず，またNASH患者の大部分が生活習慣病を背景にしているとはいえ，世界的にもevidence levelの高い臨床研究は多くはない．

そこで，第45回日本肝臓学会総会（工藤正俊会長）において，NASH（病態・診断・予後・治療）をテーマとしたコンセンサス　パネルディスカッションが日本肝臓学会として初めて催された．比較的エビデンスレベルが高く，発表者と座長のコンセンサスが得られた事項で有益な情報をInformative statementとし，推奨すべき指針をRecommendationとして取り上げた．エビデンスレベルが低いため欧米のガイドラインでは採用されていないか，発表者と座長の予備検討において全員の賛同が得られなかった事項については，アンサーパッドで学会参加者に意見を求めた．その際，回答者の2/3以上の承認が得られればConsensus Statementとして採用した（Table 2）．アンサーパッドの参加者は200人であり，内訳は内科医が88%，肝炎診療の経験年数が10年以上の医師が83%，肝臓学会専門医も83%を占めた．本稿ではその内容の大略を紹介する．

1）大阪府済生会吹田病院肝臓センター
2）高知大学消化器内科学
3）市立奈良病院消化器肝臓病センター
4）東京女子医科大学消化器内科学
5）箕面市立病院内科
6）川崎病院肝臓消化器病センター
7）山形大学消化器内科学
8）近畿大学消化器内科
*Corresponding author: saibarat@kochi-u.ac.jp
＜受付日2009年11月9日＞＜採択日2009年11月18日＞

NASHの診断アルゴリズム

NASHの診断アルゴリズムをFig. 1に示す．上述のように，NASHの診断は肝生検を用いて病理学的に行われる[6]（Table 2 Consensus statement 4，C-4）．小葉中心性に中～大滴性の脂肪滴を伴う肝細胞が出現し，小葉内の炎症細胞浸潤（好中球，リンパ球），肝細胞の風船様変性hepatocyte ballooning，Mallory-Denk体，肝細胞周囲性の線維化pericellular fibrosisや類洞に沿った線維化perisinusoidal fibrosis，巨大ミトコンドリア，好酸性壊死や鉄沈着などを伴うことが知られている．しかし，これらの病理所見がすべて観察されるNASH症例は多くない．そこで今日では組織学的に確定診断がなされたNASHに加えて，臨床的にNASHを疑ったが病理学的に単純性脂肪肝と診断された症例，さらにはNASHを基盤に発症した肝硬変や肝細胞癌をも包括する広い概念としてしばしばNAFLDという用語が用いられる．

では，どのような症例を今日的な意味でNASHと診断すべきであろうか．1999年にMatteoniらは多数のNAFLD症例を集めて肝組織像と肝疾患関連死との関係を検討し，すでに肝臓に線維化を有する症例やMallory-Denk体を有する症例，また，肝細胞に風船様変性が認められる症例では，単純性脂肪肝に比して肝疾患関連死が多いと報告し[7]，その成績はRafiqらによって再確認された[8]．これを受けて今回のミーティングでは，生命予後に悪影響を及ぼす病変を持った脂肪肝症例であることがNASHの診断に重要だとの考えに基づき，NASHの診断に際しては1）肝細胞の大滴性脂肪化，2）炎症性細胞浸潤，3）肝細胞の風船様腫大の3つの病理学所見が揃うことを必須とする共通認識が成立した（C-5）．

NAFLDはすでにNASH・NAFLDの診療ガイド[4]において，「明らかな飲酒歴がないにもかかわらず，肝組織所見はアルコール性肝障害に類似した主に大滴性の脂肪沈着を特徴とする肝障害」と定義されている．これらの症例の中から，上記の病理学的所見を指標に典型的なNASH症例を選び出すことは比較的容易である．しかし，肝生検の部位による肝組織像の差異は避けられないし[9][10]，当然のことながら十分量の肝生検組織片が必要であり，かつ一部の症例では診断がNASHと単純性脂肪肝とに病理医の間でも分かれることもある．これはNASHと診断する際にどのような病理学的所見を最も重視するか，専門医の間でも共通認識の形成が

Table 1　Ludwigによる脂肪肝炎の分類

アルコール性	NASH	
	原発性	二次性
	肥満関連	薬剤性・術後性等

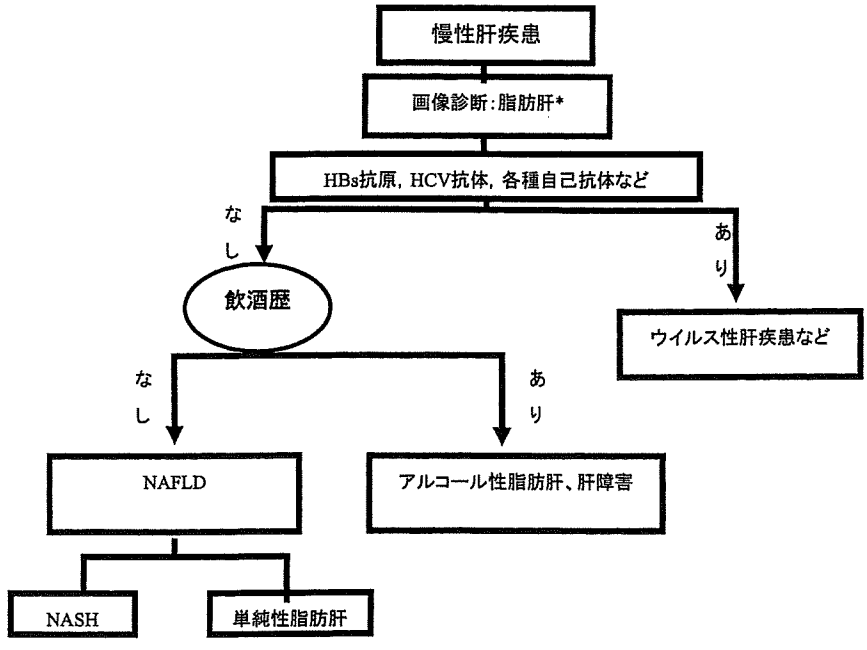

Fig. 1　NASH診断のアルゴリズム

Table 2　NASH・NAFLDに関して，今回のミーティングで合意が得られた事項

	Consensus statement	Evidence garde & level
1	NASHは肥満を誘因とする非飲酒者の慢性肝疾患である.	Level 1a/Grade A
2	非飲酒者のアルコールの摂取基準は男女ともにエタノール換算で20g/日(140g/週）未満とする.	Level 3/Grade C
3	NASH・NAFLDと診断するためには他の慢性肝疾患を除外する必要がある.	Level 1a/Grade A
4	NASH診断のGold Standardは肝生検である.	Level 1a/Grade A
5	NASHの組織学的診断には下記3項目を必須とする. 1）肝細胞の大滴性脂肪化 2）炎症性細胞浸潤 3）肝細胞の風船様腫大	Level 2b, Grade B
6	肝生検の適応となる症例を選択する基準は存在しない.	Level 3, Grade C
7	NASHを確定診断できる画像診断や臨床検査値は確立されていない.	Level 3/Grade C
8	NASHには肥満以外にも 多様な誘因が存在する. 例：消化管手術に伴うNASH等の二次性NASH	Level 1a/Grade A
9	NASH・NAFLDの発症に肥満，特に内臓脂肪型肥満が重要である.	Level 1a/Grade A
10	NASH・NAFLDの発症に2型糖尿病，特にインスリン抵抗性が重要である.	Level 1a/Grade A
11	NASH・NAFLDの発症に人種差，遺伝子多型などの遺伝的背景が重要である.	Level 2b/Grade B
12	NASH・NAFLDの発症にアディポカイン，サイトカインが重要である.	Level 4/Grade B
13	NASH・NAFLDの発症に酸化ストレス（ROS）が重要である.	Level 2b/Grade B
14	NASHを放置すれば，肝臓の線維化が進展する.	Level 3/Grade C
15	NASHの予後は一般住民の予後より不良である.	Level 2a/Grade B
16	NASHによる肝硬変は肝細胞癌の高危険群である.	Level 2a/Grade A
17	NASHにおける肝発癌の危険因子には肥満・糖尿病・肝の線維化・高齢がある.	Level 2a/Grade A
18	NASH・NAFLDの治療を行った場合には，治療効果の評価が必要である.	Level 1a/Grade A
19	NASH・NAFLDの治療の有効性の証明にはエビデンスレベルの高い検証が必要である.	Level 1a/Grade A
20	NASH・NAFLDの治療効果の評価には血清ALT値と共に肝組織像による評価が望ましい.	Level 3/Grade C
21	肥満をともなうNASH・NAFLD症例では，継続した食事・運動併用療法が有用である.	Level 3/Grade C
22	NASH・NAFLDでは肥満治療薬による治療が検討されている.	Level 4/Grade C
23	インスリン抵抗性の強いNASH・NAFLD症例の治療にはインスリン抵抗性改善薬が有用である.	Level 2a/Grade A
24	NASH・NAFLDでは抗酸化剤や瀉血による肝病態の改善が報告されている.	Level 4/Grade C
25	NASH・NAFLDでは脂質異常改善剤による肝機能の改善が報告されている.	Level 4/Grade C
26	NASH・NAFLDでは肝臓用薬による肝機能の改善が報告されている.	Level 4/Grade C
27	NASHではアンジオテンシンII 1型受容体拮抗薬の肝機能改善・線維化抑制効果が報告されている.	Level 4/Grade C
28	NASH・NAFLDでは治療標的分子の候補が明らかになりつつある.	Level 4/Grade C
29	NASH・NAFLDではQOLを損なわない臨床応用可能な治療法・治療薬の開発が望ましい.	Level 4/Grade C

	Recommendation	Evidence garde & level
1	NAFLDを疑った時，血小板低下や線維化マーカーの上昇，高齢等があれば，肝生検を考慮する.	Level 2b/Grade B
2	二次性NASHでは誘因を付記することが望ましい. 例：消化管手術に伴うNASH	Level 1a/Grade A
3	NAFLDでは発症に重要な役割を果たす肥満，特に内臓脂肪型肥満についての評価を行うことが必要である.	Level 1a/Grade A
4	NAFLDでは発症に重要な役割を果たす2型糖尿病，特にインスリン抵抗性についての評価を行うことが必要である.	Level 1a/Grade A
5	NAFLDではQOLや生命予後を低下させる要因に対する介入が必要である.	Level 2b/Grade B
6	NAFLDでは肝硬変や発癌を念頭においた治療介入と，定期検査が必要である.	Level 2b/Grade B
7	肥満をともなう症例では，継続した食事・運動併用療法を勧める.	Level 2a/Grade B
8	食事・運動併用療法による治療効果が得られない場合には，病態に応じた治療を考慮する.	Level 4/Grade C

Table 3　NASHと単純性脂肪肝の鑑別に有用性が期待されているマーカー

インスリン抵抗性
HOMA-IR
Leptin
Adiponectin
線維化
Hyaluronic acid
typeIV collagen 7S
TGFβ
酸化ストレス
TBARS
Oxidized-LDL
Total antioxidant response
Total lipid peroxide levels
Thioredoxin
炎症
TNFα
hsCRP
Ferritin
アポトーシス
CK-18 fragments
TNF-α/adiponectin ratio
Interleukin-6
CCL2
内分泌
DHEA-S

HOMA-IR：homeostasis model assessment for insulin resistance, TGFβ：transforming growth factor β, TBARS：thiobarbituric acid-reacting substance, LDL：low-density lipoprotein, TNF：tumor necrosis factor, hsCRP：high sensitivity C-reactive protein
CK：cytokeratin, CCL2：CC-chemokine ligand-2, DHEA-S：dehydroepiandrosterone-sulphate

未だ充分でないからである[11]．また，どのようなNAFLD症例を肝生検の適応とすれば効率よくNASHを発見できるかについても未だ結論が得られていない[6][12][13]（C-6）．このため，NAFLDをNASHと単純性脂肪肝と判別するための非観血的検査法や指標作りが試みられた[14]~[16]（Table 3）．しかし，NASHとの診断に至らない症例が単純性脂肪肝であり，微少な病理学的差異を鑑別する方法は未だ確立されていない（C-7）．

このミーティングでは，肥満・糖尿病・インスリン抵抗性・高齢などを伴いNAFLDが疑われる症例では，血小板数の低下や肝線維化マーカーの上昇など肝臓の線維化を疑わせる所見があれば肝生検を考慮することが推奨された[17]（Table 2 Recommendation 1，R-1）．

NASHの発症機序

NAFLDは病理学的所見から集約された症候群であり，その誘因は多様である（Table 1）（C-8）．しかし，その中心となる肥満を背景とするNAFLDはメタボリックシンドロームの肝臓における表現型であり，人種差[18]や遺伝子多型[19][20]などの遺伝的背景に加えて（C-11），肥満（特に内臓脂肪型肥満）を背景とする2型糖尿病（特にインスリン抵抗性）などの環境因子が重積して（C-9，10），酸化ストレス（ROS）[21][22]やアディポカイン，サイトカインを介した肝障害[23][24]が惹起され，発症に結びつくと考えられている（C-12，13）．このため，NAFLDの存在を疑った場合には，背景因子である内臓脂肪型肥満やインスリン抵抗性に着目した2型糖尿病の存在について評価を行うことが推奨された（R-3，4）．

NASHの自然経過と予後・肝発癌のリスク

NAFLDではQOLや生命予後を低下させる要因として，メタボリックシンドロームの合併やNASHへの進展が想定される．従って，その予後を改善するためには，生活習慣病やNASHに対する治療が必要との共通認識が得られた（C-14，15）．また，本邦では多数のNASH症例を長期に観察した報告はないが，今回のミーティングでは欧米で肝疾患関連死の増加につながると報告された肝組織像を呈する症例をNASHと規定することにより[7][8]（C-5），NASHの予後は一般住民より不良との共通認識を得ることが可能であった（C-15）．

NAFLDは明らかな飲酒歴がないにもかかわらず，肝組織所見はアルコール性肝障害に類似した主に大滴性の脂肪が主として中心静脈周囲に沈着することを特徴とする慢性肝障害である．約1割のNASH症例に加えて，今後NASHに進展する症例を含む集団であることから，放置すれば肝臓の線維化が進展すると容易に推定される．欧米の多くの論文でもNAFLDを放置すれば肝臓の線維化が進展し，肝疾患関連死の増加に繋がると報告されている[25]~[28]．しかし，意外なことに，今回のミーティングではNAFLDを放置すれば肝臓の線維化が進展するとの共通認識を得ることはできなかった．

NASHは肝硬変に進展するのみならず，肝細胞癌の温床となる[29]（C-16）．NASHにおける肝発癌のピークは70歳代にあり，進展した肝の線維化，肥満や糖尿病が肝発癌の危険因子である（C-17）．肝生検が行われる症例はNASHが疑われる症例であり，例え採取された肝組織にNASHとの診断に足る所見が得られなくとも，

Table 4　NAFLD/NASHの治療標的

肥満（内臓肥満）
インスリン抵抗性
　遊離脂肪酸
　サイトカイン，アディポサイトカイン
　　TNF-α，IL-6，アディポネクチン，etc.
　インスリンシグナル阻害因子
　　PKCs，JNK1，FOXO1，etc.
　酸化ストレス
　ERストレス，ミトコンドリアストレス
　脂肪酸代謝制御因子
脂質代謝異常
　脂肪分解（遊離脂肪酸の産生）
　　インスリン抵抗性，ホルモン感受性リパーゼ，MCP-1, TNF-α，etc.
　脂肪酸合成関連酵素
　　acetyl-CoA carboxylase1，2，etc.
　脂肪酸酸化関連酵素
　　carnitine palmitoyltranferase1，etc.
　脂肪酸代謝制御因子
　　AMPK，SREBP1，ChREBP，PPARα，γ，LXR，etc
　中性脂肪分泌関連因子
　　Microsomal triglyceride transfer protein，apoB，etc.
　脂肪滴関連因子
　　perilipinA，adipophilin，TIP47，etc.
　サイトカイン，アディポサイトカイン
　ホルモン
　　甲状腺ホルモン，女性ホルモン，成長ホルモン
　その他
　　アディポニュートリン，etc
酸化ストレス・炎症・アポトーシス
　標的細胞
　　Kupffer細胞，マクロファージ，NKT細胞，etc
　遊離脂肪酸
　ミトコンドリアストレス，ERストレス
　鉄過剰蓄積
　腸内細菌，エンドトキシン
　サイトカイン，ケモカイン，アディポサイトカイン
　　TNF-α，IL-6，IL-1β，MCP-1，アディポネクチン
　炎症，アポトーシス関連因子
　　Toll-like receptor
　　JNK，IKK，AP-1，NFκB，etc.
　　COX-2，Liopoxigenese，etc.
　　Fas/FasL，caspase，etc.
抗肝線維化
　標的細胞
　　肝星細胞，Kupffer細胞，類洞内皮細胞，etc.
　サイトカイン，ケモカイン，アディポサイトカイン，増殖因子
　　TGF-β，MCP-1，レプチン，アディポネクチン，TNF-α，
　　アンギオテンシン，FGF，CTGF，etc.
　線維化蛋白/分解因子
　　ECM，TIMP，MMP，etc.
　シグナル
　　Smad系，MAPK系，
　炎症，酸化ストレス
　転写因子，核内受容体
　　PPARγ，LXR，FXR etc.

肝生検の部位による肝組織像の差や今後NASHに進展する可能性を考慮して，慎重な経過観察が必要であることは言うまでもない．

NASHに対する治療

NASHの最大の誘因は肥満である．従って，肥満を伴う症例では，継続した食事・運動療法による減量が有用である(C-21，R-7)．すでに胃のbandingなどの外科的治療による減量の導入が始まっており，その有用性を示す報告が認められる[30]．また，肥満治療薬による治療も検討されている(C-22)．しかし，非肥満のNASHや減量が困難な症例や治療効果が充分でない症例では，病態に応じた治療を考慮する必要がある(C-23，24，25，26，R-8)(Table 4)．NASHに対して効能を有する薬物は現時点ではない[4]が，NASH研究の進歩により，治療標的分子の候補が明らかになりつつある(C-27，28)．例えば，NAFLDの発症には酸化ストレス(C-13)の関与が示唆されており，酸化ストレスの軽減を目指した抗酸化薬の投与や瀉血による肝病態の改善が報告されている(C-24)．また，インスリン抵抗性の強い症例ではインスリン抵抗性改善薬の有用性が示され(C-23)，脂質異常改善剤（C-25）や肝臓用薬（C-26）による肝機能の改善，アンジオテンシンII1型受容体拮抗薬の肝機能改善・線維化抑制効果が報告されている(C-27)．しかし，NAFLD/NASHの原因，病態は均一ではなく，各々の病因や病態に対応した治療法の開発が必要と考えられる．NASHは肝硬変，肝細胞癌へ進展し得る病態なので，NAFLDでは肝硬変や肝発癌を念頭においた治療介入と定期検査が必要である(R-5，6)．またNASH発症・進展の分子機構解明の研究の進歩により，種々

の治療標的が示されている[31]（Table 4）ので，QOLを損なわない臨床応用可能な治療法・治療薬の開発が望まれる（C-29）．さらに，何らかの治療を行った場合には治療効果の評価が必要であり（C-18），有効性の証明には信頼性の高い検証が必要である（C-19）．従って，NASHに対する治療効果の評価は血清ALT値とともに，肝組織像による評価が望ましい（C-20）．

文　献

1) Ludwig J, Viggiano TR, McGill DB, et al. Nonalcoholic steatohepatitis: Mayo Clinic experiences with a hitherto unnamed disease. Mayo Clinic Proceedings 1980; 55: 434—488
2) Schaffner F, Thaler H. Nonalcoholic fatty liver disease. Progress in Liver Disease 1986; 8: 283—298
3) Wanless IR, Lentz JS. Fatty liver hepatitis (steatohepatitis) and obesity: an autopsy study with analysis of risk factors. Hepatology 1990; 12: 1106—1110
4) 日本肝臓学会編.「NASH・NAFLDの診療ガイド」，文光堂，東京，2006，p30—31
5) Ono M, Saibara T. Clinical features of nonalcoholic steatohepatitis in Japan: Evidence from the literature. Journal of Gastroenterology 2006; 41: 725—732
6) Sanyal AJ. AGA technical review on nonalcoholic fatty liver disease. Gastroenterology 2002; 123: 1705—1725
7) Matteoni CA, Younossi ZM, Gramlich T, et al. Nonalcoholic fatty liver disease: a spectrum of clinical and pathological severity. Gastroenterology 1999; 116: 1413—1419
8) Rafiq N, Bai C, Fang Y, et al. Long-term follow-up of patients with nonalcoholic fatty liver. Clinical Gastroenterol Hepatol 2009; 7: 234—238
9) Murata Y, Ogawa Y, Saibara T, et al. Tamoxifen-induced non-alcoholic steatohepatitis in patients with breast cancer: determination of a suitable biopsy site for diagnosis. Oncol Rep 2003; 10: 97—100
10) Merriman RB, Ferrell LD, Patti MG, et al. Correlation of paired liver biopsies in morbidly obese patients with suspected nonalcoholic fatty liver disease. Hepatology 2006; 44: 874—880
11) Kleiner DE, Brunt EM, Van Natta M, et al. Design and validation of a histological scoring system for nonalcoholic fattyliver disease. Hepatology 2005; 41: 1313—1321
12) Neuschwander-Tetri BA, Caldwell SH. Nonalcoholic steatohepatitis: summary of an AASLD Single Topic Conference. Hepatology 2003; 37: 1202—1219
13) Farrell GC, Chitturi S, Lau GK, et al; Asia-Pacific Working Party on NAFLD. Guidelines for the assessment and management of non-alcoholic fatty liver disease in the Asia-Pacific region. J Gastroenterol Hepatol 2007; 22: 775—777
14) Angulo P, Hui JM, Marchesini G, et al. The NAFLD fibrosis score: a noninvasive system that identifies liver fibrosis in patients with NAFLD. Hepatology 2007; 45: 846—854
15) Harrison SA, Oliver D, Arnold HL, et al. Development and validation of a simple NAFLD clinical scoring system for identifying patients without advanced disease. Gut 2008; 57: 1441—1447
16) Guha IN, Parkes J, Roderick P, et al. Noninvasive markers of fibrosis in nonalcoholic fatty liver disease: Validating the European Liver Fibrosis Panel and exploring simple markers. Hepatology 2008; 47: 455—460
17) Vuppalanchi R, Chalasani N. Nonalcoholic fatty liver disease and nonalcoholic steatohepatitis: Selected practical issues in their evaluation and management. Hepatology 2009; 49: 306—317
18) Browning JD, Szczepaniak LS, Dobbins R, et al. Prevalence of hepatic steatosis in an urban population in the United States: impact of ethnicity. Hepatology 2004; 40: 1387—1395
19) Dong H, Wang J, Li C, et al. The phosphatidylethanolamine N-methyltransferase gene V175M single nucleotide polymorphism confers the susceptibility to NASH in Japanese population. J Hepatol 2007; 46: 915—920
20) Romeo S, Kozlitina J, Xing C, et al. Genetic variation in PNPLA3 confers susceptibility to nonalcoholic fatty liver disease. Nat Genet 2008; 40: 1461—1465
21) Sumida Y, Nakashima T, Yoh T, et al. Serum thioredoxin levels as a predictor of steatohepatitis in patients with nonalcoholic fatty liver disease. J Hepatol 2003; 38: 32—38
22) Ikura Y, Ohsawa M, Suekane T, et al. Localization of oxidized phosphatidylcholine in nonalcoholic fatty liver disease: impact on disease progression. Hepatology 2006; 43: 506—514

23) Diehl AM, Li ZP, Lin HZ, et al. Cytokines and the pathogenesis of non-alcoholic steatohepatitis. Gut 2005; 54: 303—306
24) Hui JM, Hodge A, Farrell GC, et al. Beyond insulin resistance in NASH: TNF-alpha or adiponectin? Hepatology 2004; 40: 46—54
25) Teli MR, James OF, Burt AD, et al. The natural history of nonalcoholic fatty liver: a follow-up study. Hepatology 1995; 22: 1714—1719
26) Fassio E, Alvarez E, Dominguez N, et al. Natural history of nonalcoholic steatohepatitis: a longitudinal study of repeat liver biopsies. Hepatology 2004; 40: 820—826
27) Adams LA, Sanderson S, Lindor KD, et al. The histological course of nonalcoholic fatty liver disease: a longitudinal study of 103 patients with sequential liver biopsies. J Hepatol 2005; 42: 132—138
28) Ekstedt M, Franz L E, Mathiesen U L, et al. Long-Term Follow-up of Patients With NAFLD and Elevated Liver Enzymes. Hepatology 2006; 44: 865—873
29) Shimada M, Hashimoto E, Taniai M, et al. Hepatocellular carcinoma in patients with non-alcoholic steatohepatitis. J Hepatol 2002; 37: 154—160
30) Mummadi RR, Kasturi KS, Chennareddygari S, et al. Effect of bariatric surgery on nonalcoholic fatty liver disease: systematic review and meta-analysis. Clin Gastroenterol Hepatol 2008; 6: 1396—1402
31) Anderson N, Borlak J. Molecular Mechanisms and therapeutic targets in steatosis and steatohepatitis. Pharmacol Rev 2008; 60: 311—357

JSH Consensus Kobe 2009; Diagnosis and Treatment of NASH

Takeshi Okanoue[1], Toshiji Saibara[2]*, Masafumi Ono[2], Yoshio Sumida[3], Etsuko Hashimoto[4], Shinji Tamura[5], Gotaro Yamada[6], Sumio Kawada[7], Masatoshi Kudo[8]

Key words: oxidative stress　insulin resistance　metabolic syndrome　liver cirrhosis　hepatocellular carcinoma

Kanzo 2009; 50: 741—747

1) Saiseikai Suita Hospital
2) Kochi University
3) Nara City Hospital
4) Tokyo Women's Medical School
5) Mino City Hospital
6) Kawasaki Hospital
7) Yamagata University
8) Kinki University
*Corresponding author: saibarat@kochi-u.ac.jp

LIVER TRANSPLANTATION 15:806-809, 2009

ORIGINAL ARTICLE

Recurrent Familial Hypobetalipoproteinemia-Induced Nonalcoholic Fatty Liver Disease After Living Donor Liver Transplantation

Noboru Harada,[1] Yuji Soejima,[1] Akinobu Taketomi,[1] Tomoharu Yoshizumi,[1] Hideaki Uchiyama,[1] Toru Ikegami,[1] Toshiharu Saibara,[2] Takashi Nishizaki,[3] and Yoshihiko Maehara[1]

[1]Department of Surgery and Medical Science, Graduate School of Medical Sciences, Kyushu University, Fukuoka, Japan; [2]Department of Gastroenterology and Hepatology, Kochi University, Kochi, Japan; and [3]Department of Surgery, Matsuyama Red Cross Hospital, Matsuyama, Japan

Familial hypobetalipoproteinemia (FHBL) is one of the causes of nonalcoholic steatohepatitis (NASH) and a codominant disorder. Patients heterozygous for FHBL may be asymptomatic, although they demonstrate low plasma levels of low-density lipoprotein (LDL) cholesterol and apolipoprotein B. Here we report a nonobese 54-year-old man with decompensated liver cirrhosis who underwent living donor liver transplantation with his son as the donor. Low albuminemia and refractory ascites persisted after transplantation. A biopsy specimen obtained 11 months after liver transplantation revealed severe steatosis and fibrosis, and recurrent NASH was diagnosed on the basis of pathological findings. Both the patient's and donor's laboratory tests demonstrated low LDL cholesterol and apolipoprotein levels. Because mutations in messenger RNAs of microsomal triglyceride transfer protein and apolipoprotein B genes were excluded neither in the recipient nor in the donor, both were clinically diagnosed as being heterozygous for FHBL. We successfully treated the recipient with heterozygous FHBL–induced recurrent NASH after liver transplantation using our diet and exercise programs. *Liver Transpl 15:806-809, 2009.*

Received 12 December 2008; accepted 20 January 2009.

Cryptogenic cirrhosis is one of the most common indications for liver transplantation. Several possible causes of cryptogenic cirrhosis have been suggested, including occult alcohol abuse, occult viral infection, silent autoimmune hepatitis, and burned-out nonalcoholic fatty liver disease (NAFLD), and this depends in part on the vigor of the diagnostic efforts.[1] Because a subgroup of patients with NAFLD can progress to cirrhosis,[2] it is possible that nonalcoholic steatohepatitis (NASH) may be an important cause of cryptogenic cirrhosis and an indication for liver transplantation. However, NASH has been reported to recur occasionally among patients with cryptogenic cirrhosis after orthotopic liver transplantation.[3]

Abetalipoproteinemia, a homozygous deficiency of the microsomal triglyceride transfer protein (MTP) gene, results in massive hepatic steatosis and liver cirrhosis.[4] Familial hypobetalipoproteinemia (FHBL) is classified as one of the causes of NAFLD, and its frequency in the heterozygous form has been estimated with clinical criteria to be 1:500 to 1:1000.[4] Thus, homozygous FHBL is an exceedingly rare disease but results in extremely low serum levels of low-density lipoprotein (LDL) cholesterol and apolipoprotein B similar to those observed in abetalipoproteinemia. Therefore, children with homozygous FHBL often have hepatic steatosis and, less frequently, severe clinical manifestations such as failure to thrive and intestinal fat malabsorption.[5] In con-

Abbreviations: γ-GTP, gamma-glutamyl transpeptidase; Alb, albumin; ALP, alkaline phosphatase; ALT, alanine aminotransferase; AST, aspartate aminotransferase; Bx, biopsies; FHBL, familial hypobetalipoproteinemia; HBL, hypobetalipoproteinemia; LDL, low-density lipoprotein; MTP, microsomal triglyceride transfer protein; NAFLD, nonalcoholic fatty liver disease; NASH, nonalcoholic steatohepatitis; PCSK9, proprotein convertase subtilisin/kexin type 9; T-Bil, total bilirubin.

Address reprint requests to Noboru Harada, M.D., Department of Surgery and Medical Science, Graduate School of Medical Sciences, Kyushu University, 3-1-1 Maidashi, Higashi-ku, Fukuoka 812-8582, Japan. Telephone: 81-92-642-5466; FAX: 81-92-642-5482;
E-mail: nharada@surg2.med.kyushu-u.ac.jp

DOI 10.1002/lt.21766
Published online in Wiley InterScience (www.interscience.wiley.com).

trast, heterozygous FHBL may be asymptomatic, with subjects identified by population screening for low serum cholesterol or presenting with clinical manifestations that require medical attention. Fatty liver disease with mild elevations of serum liver enzymes is the main clinical manifestation, but oral fat intolerance and intestinal fat malabsorption have occasionally been reported in some patients.[4]

In this report, we describe a NASH patient with cryptogenic cirrhosis who underwent living donor liver transplantation using a hepatic graft from his son. NASH recurred unexpectedly after liver transplantation, and an investigation based on both clinical and genetic analysis revealed that this patient and his son were suffering from heterozygous FHBL. This could be an unusual manifestation in heterozygous FHBL, but such a case should be taken into account in the treatment of heterozygous FHBL.

CASE REPORT

A 54-year-old thin male was diagnosed with liver dysfunction by a medical examination and admitted to the local hospital. His height, weight, and body mass index were 172 cm, 56.8 kg, and 19.2 kg/m^2, respectively. Laboratory tests revealed elevated aspartate aminotransferase (AST; 64 U/L), alanine aminotransferase (ALT; 85 U/L), gamma-glutamyl transpeptidase (γ-GTP; 477 IU/L), alkaline phosphatase (ALP; 505 IU/L), and serum glucose (144 mg/dL) levels; a slightly elevated total bilirubin level (1.6 mg/dL); normal total cholesterol (136 mg/dL), triglyceride (72 mg/dL), and high-density lipoprotein cholesterol (65 mg/dL) levels; and a low platelet count (92,000/μL). He consumed approximately 350 mL of beer per day between the ages of 20 and 50 years. He had no history of obesity when he was young. Endoscopic retrograde cholangiopancreatography could not confirm the diagnosis. Computerized tomography showed a cirrhotic pattern, massive ascites, and moderate splenomegaly. Viral infections (hepatitis B virus, hepatitis C virus, and cytomegalovirus), metabolic diseases (Wilson disease, hemochromatosis, and alpha-1-antitrypsin disease), and cholestatic liver disease (primary biliary cirrhosis and primary sclerosing cholangitis) were excluded. A pathological examination of the liver biopsy specimen showed partly degenerative foci and fatty changes in the distorted lobular areas, mild-to-moderate chronic inflammatory infiltrated cells and mild piecemeal necrosis were found in the enlarged fibrous portal tracts, and occasional hepatocytes containing Mallory bodies were observed. On the basis of these findings, he was diagnosed with decompensated cryptogenic cirrhosis and refractory ascites, which is an indication for liver transplantation. NASH was highly suspected but was not confirmed before the transplantation surgery.

The donor candidate was the patient's 28-year-old son, whose blood type was identical to that of his father (B+). The donor's height, weight, and body mass index were 174.5 cm, 100 kg, and 32.8 kg/m^2, respectively, and he had no history of alcohol consumption. Preoperative laboratory tests revealed elevated AST (36 U/L), ALT (61 U/L), γ-GTP (224 IU/L), and ALP (473 IU/L) levels, a normal total cholesterol level (136 mg/dL), and a normal triglyceride level (72 mg/dL). Because an ultrasound examination revealed a hyperechogenic liver suggesting significant steatosis, we prescribed a diet and exercise regimen. The diet[6] included 1000 kcal of food, running for approximately 5 km per day, and the administration of both 400 mg of bezafibrate and 300 mg of ursodeoxycholic acids. After 30 days, his weight had decreased to 80 kg, and an ultrasound scan showed improvement of the steatotic liver. We obtained a liver biopsy specimen, and a pathological examination (Fig. 1A) showed mild macrovesicular steatosis without inflammation or fibrosis around the portal area. The extent of macrovesicular steatosis of the liver biopsy specimen was less than 10%. We therefore determined that he could serve as the donor. He volunteered to donate his left hepatic lobe.

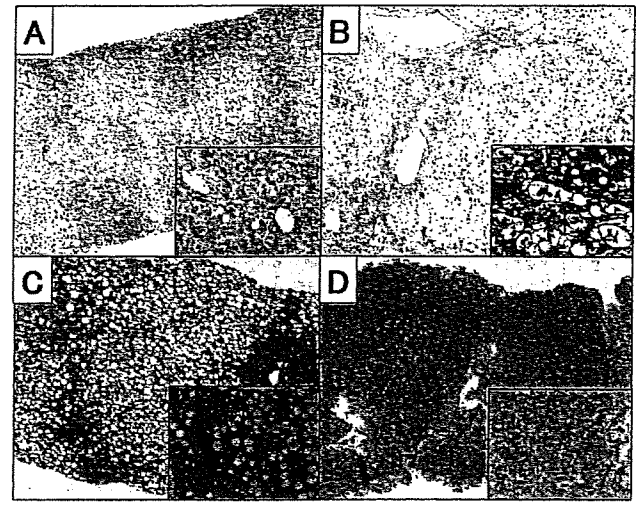

Figure 1. (A) Donor's liver biopsy. Ten percent of the macrovesicular steatosis was found after a strict diet and exercise program (hematoxylin-eosin stain; original magnification, ×100). The inset is a high magnification (×400) of the liver biopsy specimen. (B) Explanted liver pathology (hematoxylin-eosin stain; original magnification, ×100). Mild fatty changes, chronic inflammatory infiltrated cells, and piecemeal necrosis were found in the fibrous enlarged portal areas. The inset is a high magnification (×400) of the liver biopsy specimen. The arrows indicate Mallory bodies. (C) Liver biopsy at postoperative day 330 after liver transplantation (hematoxylin-eosin stain; original magnification, ×100). Severe macrovesicular steatosis (>50%) was found. The inset is a high magnification (×400) of the liver biopsy specimen. The arrows indicate Mallory bodies. (D) Liver biopsy at postoperative day 575 after liver transplantation (hematoxylin-eosin stain; original magnification, ×100). There was almost no steatosis. The inset is a high magnification (×400) of the liver biopsy specimen.

The patient underwent living donor liver transplantation on July 11, 2005. The graft weight was 380 g, which accounted for 31.0% of the standard liver volume of the recipient. Immunosuppression consisted of tacrolimus, prednisone, and mycophenolate mofetil. On the pathological examination of the explanted liver (Fig.

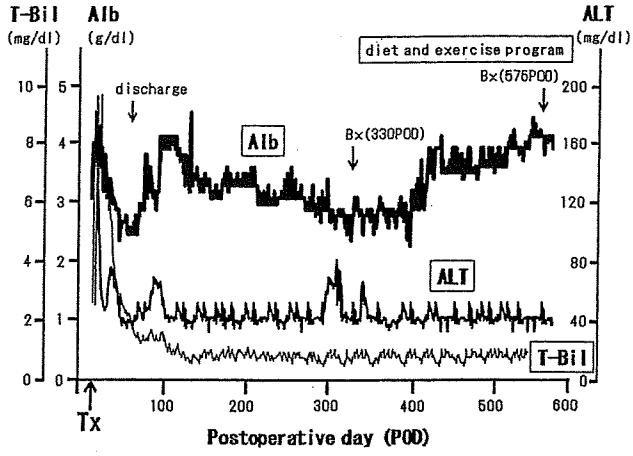

Figure 2. Postoperative course. Laboratory test data, including serum total bilirubin (T-Bil; thin black line), serum albumin (Alb; bold black line), and serum alanine aminotransferase (ALT; bold gray line), are shown. Liver biopsies (Bx) were performed at postoperative days 330 and 575.

1B), mild fatty changes were seen in the distorted lobular areas. Mild-to-moderate chronic inflammatory cells and mild piecemeal necrosis were detected in the fibrous enlarged portal areas, and occasional hepatocytes containing Mallory bodies were observed, which were consistent with the diagnosis of NASH. The early postoperative course was uneventful except for serum hyperglycemia (Fig. 2). However, he gradually demonstrated low albuminemia (2.5 g/dL) and refractory ascites (2000 mL/day). Neither acute cellular rejection nor acute cholangitis developed, and ascites gradually decreased. The patient was finally discharged on postoperative day 57 (Fig. 2).

Eleven months after liver transplantation, he began experiencing general fatigue and developed steatorrhea, and he demonstrated moderate liver dysfunction. He had not consumed any alcohol after liver transplantation. Laboratory tests revealed elevated AST (45 U/L), ALT (28 U/L), γ-GTP (177 IU/L), and ALP (1083 IU/L) levels and normal total cholesterol (115 mg/dL) and triglyceride (65 mg/dL) levels. An examination of the biopsy specimen (Fig. 1C) revealed typical NASH with severe macrovesicular steatosis (>50%), Mallory bodies, and fibrosis in the transplanted liver. Moreover, both the patient's and donor's laboratory tests demonstrated hypoapolipoproteinemia. The donor's liver function tests revealed an almost normal liver.

An analysis of the apolipoprotein composition 11 months after liver transplantation revealed the following findings for the recipient: apolipoprotein A-1, 117 (105-184) mg/dL; apolipoprotein A-2, 38 (26-46) mg/dL; apolipoprotein B, 40 (38-104) mg/dL; apolipoprotein C-2, 1.1 (1.2-6.4) mg/dL; apolipoprotein C-3, 4.0 (4.2-14.5) mg/dL; and apolipoprotein E, 2.6 (3.3-5.8) mg/dL. For the donor, the following was found: apolipoprotein A-1, 137 mg/dL; apolipoprotein A-2, 27 mg/dL; apolipoprotein B, 57 mg/dL; apolipoprotein C-2, 0.1 mg/dL; and apolipoprotein E, 2.0 mg/dL. The LDL cholesterol levels were 43% for the recipient and 44% for the donor (44%-69%). Consequently, the recurrence of FHBL-induced NASH after living donor liver transplantation was noted with the observation of hypoapolipoproteinemia with low LDL cholesterol, steatorrhea, and severe macrovesicular hepatic steatosis.

The messenger RNA analysis revealed no mutations in MTP or apolipoprotein B genes. The patient was on a strict diet, which included low-fat meals and an exercise program containing 30 minutes of walking per day. Eight months after the diet was started, his general condition markedly improved, his laboratory tests revealed normal transaminases and increased albumin (3.6 mg/dL), and the ultrasound examination demonstrated a normal liver without steatosis. His laboratory tests markedly improved: AST, 21 U/L; ALT, 16 U/L; γ-GTP, 71 IU/L; ALP, 644 IU/L; total cholesterol level, 126 mg/dL; and triglyceride level, 58 mg/dL. Follow-up liver biopsy on postoperative day 575 showed almost no signs of steatosis (Fig. 1D).

DISCUSSION

Hypobetalipoproteinemia (HBL) is defined by <5th percentile serum levels of total cholesterol (<150 mg/dL), LDL cholesterol (<44%), or total apolipoprotein B (<50 mg/dL).[5] The recipient's data met all these criteria for HBL in total cholesterol, LDL cholesterol, and total apolipoprotein B. The donor's data met 2 of the criteria, total cholesterol and LDL cholesterol, although he was obese. In addition, typical clinical manifestations of HBL, such as steatorrhea and fatty liver, were observed in the recipient. Moreover, the donor's 3 children demonstrated liver dysfunction. Therefore, the recipient was clinically diagnosed as having FHBL with autosomal dominant traits. Intestinal fat malabsorption such as that seen in chronic pancreatitis, severe liver disease, malnutrition, and hyperthyroidism also may result in low apolipoprotein and cholesterol levels, and these are regarded as secondary causes of HBL. In this patient, secondary HBL was excluded by the preoperative tests.

Abetalipoproteinemia is thought to be due to a variety of genetic defects in MTP.[7] In most cases of HBL, the genetic causes are not known.[8] The best characterized cases are due to mutations of the apolipoprotein B gene, namely missense and flame-shift mutations specifying the production of truncated protein.[9] In this patient, mutations in messenger RNAs of MTP and apolipoprotein B genes were excluded, but mutations of the proprotein convertase subtilisin/kexin type 9 (PCSK9) gene causing a loss of function of the encoded protein, a proprotein convertase that regulates the LDL receptor number in the liver, were not analyzed because PCSK9 mutations do not result in fatty liver disease.[10] The donor has HBL, and he may be at risk to demonstrate steatohepatitis in the future, although missense, flame-shift, and deletion mutations in MTP and apolipoprotein B genes were excluded. There is no family history of liver dysfunction without the donor's 3 children, who have liver dysfunction and may also be at risk to develop FHBL. No follow-up prospective studies on the

progression of fatty liver toward more severe chronic liver diseases such as steatohepatitis, fibrosis, and cirrhosis have been conducted in individuals with genotyped FHBL. Therefore, liver dysfunction in the recipient, the donor, and the donor's children will need to be strictly monitored to identify a potentially progressive course.

In this case, the recipient was diagnosed preoperatively with cryptogenic cirrhosis despite vigorous diagnostic efforts. In retrospect, we concluded that he had burned-out NASH because the explanted liver pathology demonstrated inflammation, fibrosis, and Mallory bodies, which are typical characteristics of NASH. Additionally, it has been reported that NASH can recur after orthotopic liver transplantation.[3] On the basis of these findings, we diagnosed severe recurrent NASH after liver transplantation in this patient with HBL-induced nonalcoholic fatty liver cirrhosis.

A low-fat diet and exercise program proved to be effective for this patient. The fat-controlled, nutritionally adequate diet decreased the macrovesicular steatosis observed on the pathological examination, but it is not known how best to achieve improvements in steatosis of the hepatic graft. Exercise programs have been shown to be associated with better blood pressure, blood glucose, and lipid levels.[11] Therefore, it has been suggested that the metabolic calorie expenditure achieved by exercise might be effective for NASH after liver transplantation. Although our patient had insulin resistance, weight control and insulin therapy were effective in his case. There have been several pilot studies on pharmacological intervention with pioglitazone,[12] metformin,[13] nateglinide,[14] and peroxisome proliferator activated receptor-γ[15] for NASH. It has been reported that metformin should be considered a method of treatment for NASH in the transplanted liver if other treatment methods fail.[16] On the other hand, pioglitazone has been linked to hepatotoxicity after liver transplantation. Therefore, we will need to carefully choose the pharmacotherapy for this patient if he manifests liver injury due to steatohepatitis with hepatic graft fibrosis.

In conclusion, we have presented a case of severe recurrent NASH after liver transplantation using the graft of a related donor who has HBL in an FHBL-induced NASH patient with liver cirrhosis. Because burned-out NASH without any sign of hepatic steatosis or ballooned hepatocytes is classified as cryptogenic cirrhosis, the post–liver transplantation liver biopsy specimens of patients with cryptogenic cirrhosis should be carefully assessed for the development of pathological features of recurrent NASH and monitored for a potentially progressive course. In addition, a related donor who is a candidate for a patient with cryptogenic liver cirrhosis should be carefully assessed preoperatively from the perspective of heterozygous FHBL.

REFERENCES

1. Caldwell SH, Oelsner DH, Iezzoni JC, Hespenheide EE, Battle EH, Driscoll CJ. Cryptogenic cirrhosis: clinical characterization and risk factors for underlying disease. Hepatology 1999;29:664-669.
2. Matteoni CA, Younossi ZM, Gramlich T, Boparai N, Liu YC, McCullough AJ. Nonalcoholic fatty liver disease: a spectrum of clinical and pathological severity. Gastroenterology 1999;116:1413-1419.
3. Kim WR, Poterucha JJ, Porayko MK, Dickson ER, Steers JL, Wiesner RH. Recurrence of nonalcoholic steatohepatitis following liver transplantation. Transplantation 1996; 27:1802-1805.
4. Linton MF, Farese RV, Young SG. Familial hypobetalipoproteinemia. J Lipid Res 1993;34:521-541.
5. Schonfeld G. Familial hypobetalipoproteinemia: a review. J Lipid Res 2003;44:878-883.
6. Nakamuta M, Morizono S, Soejima Y, Yoshizumi T, Aishima S, Takasugi S, et al. Short-term intensive treatment for donors with hepatic steatosis in living-donor liver transplantation. Transplantation 2005;80:608-612.
7. Wetterrau JR, Aggerbeck LP, Bouma ME, Eisenberg C, Munck A, Hermier M, et al. Absence of microsomal triglyceride transfer protein in individuals with abetalipoproteinemia. Science 1992;258:999-1001.
8. Berriot-Varoqueaux N, Dannoura AH, Moreau A, Verthier N, Sassolas A, Cadiot G, et al. Apolipoprotein B48 glycosylation in abetalipoproteinemia and Anderson's disease. Gastroenterology 2001;121:1101-1108.
9. Schonfeld G. The hypobetalipoproteinemia. Annu Rev Nutr 1995;15:23-34.
10. Tarugi P, Averna M, Di Leo E, Cefalù AB, Noto D, Magnolo L, et al. Molecular diagnosis of hypobetalipoproteinemia: an ENID review. Atherosclerosis 2007;195:e19–e27.
11. Painter P, Krasnoff J, Paul SM, Ascher NL. Physical activity and health-related quality of life in liver transplant recipients. Liver Transpl 2001;7:213-219.
12. Promrat K, Lutchman G, Uwaifo GI, Freedman RJ, Soza A, Heller T, et al. A pilot study of pioglitazone treatment for nonalcoholic steatohepatitis. Hepatology 2004;39:188-196.
13. Marchesini G, Brizi M, Bianchi G, Tomassetti S, Zoli M, Melchionda N. Metformin in non-alcoholic steatohepatitis. Lancet 2001;358:893-894.
14. Morita Y, Ueno T, Sasaki N, Tateishi Y, Nagata E, Kage M, Sata M. Nateglinide is useful for nonalcoholic steatohepatitis (NASH) patients with type 2 diabetes. Hepatogastroenterology 2005;52:1338-1343.
15. Ye JM, Iglesias MA, Watson DG, Ellis B, Wood L, Jensen PB, et al. PPARalpha/gamma ragaglitazar eliminates fatty liver and enhances insulin action in fat-fed rats in the absence of hepatomegaly. Am J Physiol Endocrinol Metab 2003;284:E531–E540.
16. Jankowska I, Socha P, Pawlowska J, Teisseyre M, Gliwicz D, Czubkowski P, et al. Recurrence of non-alcoholic steatohepatitis after liver transplantation in a 13-year-old boy. Pediatr Transplant 2007;11:796-798.

THE JOURNAL OF BIOLOGICAL CHEMISTRY VOL. 284, NO. 32, pp. 21165–21176, August 7, 2009

Proanthocyanidin from Blueberry Leaves Suppresses Expression of Subgenomic Hepatitis C Virus RNA*[S]

Received for publication, April 6, 2009, and in revised form, June 12, 2009 Published, JBC Papers in Press, June 16, 2009, DOI 10.1074/jbc.M109.004945

Masahiko Takeshita[‡], Yo-ichi Ishida[§], Ena Akamatsu[§], Yusuke Ohmori[¶], Masayuki Sudoh[¶], Hirofumi Uto[‖], Hirohito Tsubouchi[‖], and Hiroaki Kataoka[1]**

*From the [‡]Research Division, Minami Nippon Dairy Co-op Co., Ltd., Miyazaki 885-0073, the [§]Miyazaki Prefectural Industrial Support Foundation, Miyazaki 880-0303, the [¶]Kamakura Research Laboratories, Chugai Pharmaceutical Co., Ltd., Kanagawa 247-8530, the [‖]Department of Digestive Disease and Life-style Related Disease, Health Research Human and Environmental Sciences, Kagoshima University, Graduate School of Medicine and Dental Sciences, Kagoshima 890-8520, and the **Section of Oncopathology and Regenerative Biology, Department of Pathology, Faculty of Medicine, University of Miyazaki, Miyazaki 889-1692, Japan*

Hepatitis C virus (HCV) infection is a major cause of chronic liver disease such as chronic hepatitis, cirrhosis, and hepatocellular carcinoma. While searching for new natural anti-HCV agents in agricultural products, we found a potent inhibitor of HCV RNA expression in extracts of blueberry leaves when examined in an HCV subgenomic replicon cell culture system. This activity was observed in a methanol extract fraction of blueberry leaves and was purified by repeated fractionations in reversed-phase high-performance liquid chromatography. The final purified fraction showed a 63-fold increase in specific activity compared with the initial methanol extracts and was composed only of carbon, hydrogen, and oxygen. Liquid chromatography/mass-ion trap-time of flight analysis and butanol-HCl hydrolysis analysis of the purified fraction revealed that the blueberry leaf-derived inhibitor was proanthocyanidin. Furthermore, structural analysis using acid thiolysis indicated that the mean degree of polymerization of the purified proanthocyanidin was 7.7, consisting predominantly of epicatechin. Proanthocyanidin with a polymerization degree of 8 to 9 showed the greatest potency at inhibiting the expression of subgenomic HCV RNA. Purified proanthocyanidin showed dose-dependent inhibition of expression of the neomycin-resistant gene and the NS-3 protein gene in the HCV subgenome in replicon cells. While characterizing the mechanism by which proanthocyanidin inhibited HCV subgenome expression, we found that heterogeneous nuclear ribonucleoprotein A2/B1 showed affinity to blueberry leaf-derived proanthocyanidin and was indispensable for HCV subgenome expression in replicon cells. These data suggest that proanthocyanidin isolated from blueberry leaves may have potential usefulness as an anti-HCV compound by inhibiting viral replication.

Hepatitis C virus (HCV)[2] is often associated with the development of chronic liver diseases. Infection by HCV causes chronic hepatitis at high rates and finally results in liver cirrhosis and subsequent occurrence of hepatocellular carcinoma (1–3). The number of people worldwide who are infected by HCV is estimated to be over 200 million with 2 million infections in Japan (4). The South Kyushu area of Japan, including Miyazaki prefecture, has a high prevalence of this virus, and it is now recognized as a social problem. There is no vaccine effective for HCV at present. The elimination of HCV may be achieved by a combination of pegylated α-interferon and ribavirin, a broad spectrum antiviral drug (4–6). However, virological response to this combination therapy has been reported to be 80% for genotypes 2 and 3, but less than 50% for genotype 1 (7, 8). Moreover, α-interferon is associated with severe side-effects, including leucopenia, thrombocytopenia, depression, fatigue, and flu-like symptoms, and ribavirin is associated with side-effects such as hemolytic anemia (9). Therefore, establishment of a new modality of treatment without serious adverse effects is still required.

Considering the prolonged period (20–30 years) required for development of liver cirrhosis and hepatocellular carcinoma in individuals infected with HCV, we speculated that progression of the disease might be influenced by daily diet. Our research project focuses on the daily use of agricultural products that could cure or reduce the risk of disease progression by HCV. Thus, we screened local agricultural products (1700 samples from 283 species) for their suppressive activity against HCV subgenome expression using an HCV replicon cell system. We found a significant suppressive activity in extracts of blueberry leaves. Blueberries are classified in the genus *Vaccinium*, and the species are native only to North America. Blueberry leaves have high quinic acid and chlorogenic acid contents and also significant flavonol glycosides such as rutin. Thus, they are high in antioxidant activity. In our subsequent screening studies using various kinds of blueberry species, the most potent activity was observed in the leaf of rabbit-eye blueberry (*Vaccinium virgatum* Aiton), which is cultivated in southern areas of Japan.

* This study was supported by a grant from the Collaboration of Regional Entities for the Advancement of Technological Excellence (CREATE) from Japan Science and Technology Agency.

[S] The on-line version of this article (available at http://www.jbc.org) contains supplemental Figs. S1–S3.

[1] To whom correspondence should be addressed: Section of Oncopathology and Regenerative Biology, Dept. of Pathology, Faculty of Medicine, University of Miyazaki, 5200 Kihara, Kiyotake, Miyazaki 889-1692, Japan. Tel.: 81-985-85-2809; Fax: 81-985-85-6003; E-mail: mejina@fc.miyazaki-u.ac.jp.

[2] The abbreviations used are: HCV, hepatitis C virus; hnRNP, heterogeneous nuclear ribonucleoprotein; HPLC, high-performance liquid chromatography; PDA, photodiode array; EPMA, electron probe micro-analysis; LC/MS-IT-TOF, liquid chromatography/mass spectrometry-ion trap-time of flight; APCI, atmospheric pressure chemical ionization; mDP, mean degree of polymerization; IC_{50}, concentration required for 50% inhibition; CC_{50}, concentration required for 50% cytotoxicity; eIF3, eukaryotic translation initiation factor 3; CHAPS, 3-[(3-cholamidopropryl)dimethylammonio]-1-propane sulfonate; IRES, internal ribosome entry site; DIGE, differential gel electrophoresis.

In this study, extracts of rabbit-eye blueberry leaves were used in an effort to purify and identify the compound responsible for inhibition of the expression of subgenomic HCV RNA. We identified oligomeric proanthocyanidin with mean degree of polymerization (mDP) around eight as an inhibitor of HCV subgenome expression. We also analyzed cellular proteins that have affinity to the oligomeric proanthocyanidin in HCV replicon cells and identified heterogeneous nuclear ribonucleoprotein (hnRNP) A2/B1 as one of candidate proteins involved in the proanthocyanidin-mediated inhibition of HCV subgenome expression.

EXPERIMENTAL PROCEDURES

Extraction of Blueberry Leaves—A lyophilized powder made from leaves of rabbit-eye blueberry (*V. virgatum* Aiton) was provided by Unkai Shuzo Co., Ltd. (Miyazaki, Japan). One gram of the lyophilized powder was extracted with 100 ml of methanol at room temperature with shaking for 15 min, and the supernatant was passed through filter paper (filter paper No.2, Toyo, Tokyo, Japan). The methanol extract was then extracted with 100 ml of chloroform, followed by centrifugation (1750 × *g* for 10 min), and the resultant precipitate and supernatant were collected. The precipitate was dissolved in methanol, concentrated *in vacuo*, and lyophilized (CMW-ppt). The supernatant was mixed with 150 ml of distilled water and methanol to perform a liquid-liquid extraction, and the water layer was collected and mixed with 150 ml of chloroform to repeat the chloroform extraction. The water layer was concentrated and lyophilized (CMW-W). The chloroform layer was also concentrated and lyophilized (CMW-C). Most HCV subgenome-expression inhibitory activity was recovered in the CMW-W fraction.

Preparative Fractionation by HPLC—To separate the components in the CMW-W fraction processing inhibitory activity against HCV RNA expression, we performed HPLC (Prominence System, Shimadzu, Kyoto, Japan). Preliminary fractionation of CMW-W to confirm the elution pattern of HCV expression suppressive components was carried out on a reversed-phase column (Atlantis dC18, 4.6 mm × 150 mm, 3 μm, Waters, Milford, MA) at 40 °C with UV detection at 254 nm. A gradient consisting of eluant A (0.05% trifluoroacetic acid) and eluant B (acetonitrile) was applied at a flow rate of 0.7 ml/min as follows: 15–25% B linear from 0 to 12.5 min, 25–100% B linear from 12.5 to 17.5 min followed by washing 100% B from 17.5 to 25 min. For purification, the first HPLC fractionation was performed on a reversed-phase column (Atlantis T3, 4.6 mm × 150 mm, 3 μm, Waters). A gradient consisting of eluant A and eluant B (acetonitrile) was applied at a flow rate of 0.7 ml/min as follows: 30% B from 0 to 7.5 min, 30–100% B linear gradient from 7.5 to 12.5 min, followed by washing with 100% B from 12.5 to 20 min. The CMW-W fraction dissolved in 30 ml of methanol was injected, and the eluted fractions (2.1 to 18.0 min, total 26 fractions) were collected. The gradient program for the second fractionation was 20% B from 0 to 7.5 min, 20–100% B linear from 7.5 to 12.5 min, followed by washing with 100% B from 12.5 to 20 min. Fractionation of the eluate was the same as the first HPLC program. In the third HPLC fractionation, the eluant B was replaced by methanol and eluted with 40–65% B linear gradient from 0 to 12.5 min and 65–100% B linear gradient from 12.5 to 17.5 min. Fractions eluted from 2.2 to 17.5 min (total 26 fractions) were collected. In all experiments, suppressive activity of each fraction against HCV RNA expression was measured using replicon cells.

HCV Replicon Cells and Replicon Assay—The Huh-7/3-1 cell line carrying an HCV-replicon was used (10). The line was established from Huh-7 cells by stable transfection with subgenomic selectable RNA in which the encoding HCV structural proteins were replaced by the firefly luciferase gene, the internal ribosome entry site (IRES) of the *Encephalomyocarditis* virus and the neomycin phosphotransferase gene. With this HCV subgenome, the efficiency of subgenomic HCV expression could be estimated by measuring luciferase activity in the replicon cells. The HCV replicon cells were routinely grown in Dulbecco's modified Eagle's medium supplemented with Glutamax (Invitrogen), 10% fetal bovine serum, 1% penicillin/streptomycin (Invitrogen), and 500 μg/ml G418 (Invitrogen). Cells were maintained at 37 °C in a humidified atmosphere containing 5% CO_2. For the HCV subgenome expression assay, the replicon cells in Dulbecco's modified Eagle's medium supplemented with Glutamax and 5% fetal bovine serum were seeded in 96-well plates (5000 cells/well) and incubated for 24 h. Then the cells were cultured with various concentrations of samples for 72 h. Quantification of the luciferase activity was performed using the Steady-Glo Luciferase Assay System (Promega, Madison, WI) according to the manufacturer's instructions, and the luminescence was measured by DTX 800 Multimode Detector (Beckman Coulter, Fullerton, CA). The inhibitory activity was expressed as the concentration required for 50% inhibition (IC_{50}). Specific activity was calculated as a reciprocal number of IC_{50} ($1/IC_{50}$). Total activity was calculated by multiplying yielded weight by specific activity.

The cytotoxicity of the samples was measured by Cell Counting Kit-8 (Dojindo Molecular Technologies, Kumamoto, Japan) according to the manufacturer's instructions. Briefly, 10 μl/well of Cell Counting Kit-8 reagent was added to the cells cultured in a 96-well plate, incubated at 37 °C for 60 min. The absorbance of each well was measured at 450 nm with a reference wavelength at 650 nm using an Emax Precision microplate reader (Molecular Devices Inc., Sunnyvale, CA). Cell viability was calculated as relative index of control cells, and effects of samples on cell viability were expressed as the concentration required for 50% cytotoxicity (CC_{50}).

Constitutive Analysis of Electron Probe Micro-analysis and Liquid Chromatography/Mass Spectrometry-ion Trap-time of Flight (LC/MS-IT-TOF)—For electron probe micro-analysis (EPMA-1600, Shimadzu), the excitation voltage and the beam current were kept at 15 kV and at 100 nA, respectively. The diameter of the electron beam was 50 μm, and the sample was processed for carbon shadowing in advance.

Identification of the anti-HCV compound purified from blueberry leaves was done by HPLC-MSn fragmentation analyses. An HPLC System (Prominence System, Shimadzu) on a reversed-phase column (Atlantis T3, 2.1-mm inner diameter × 100 mm, 3 μm, Waters) was equipped with a photodiode array (PDA) detector scanning from 200 to 800 nm and mass spectrometry-ion trap-time of flight (MS-IT-TOF, Shimadzu)

detector. The mobile phase consisted of a gradient system 30 min of eluant A (0.05% trifluoroacetic acid) and eluant B (acetonitrile) at a flow rate of 0.25 ml/min. The elution program was 10–25% B linear from 0 to 7.5 min, 25–100% B linear from 7.5 to 12.5 min, followed by washing 100% B from 12.5 to 20 min. The column was maintained at 40 °C. Electrospray ionization conditions were recorded from m/z = 200 to 1500 in a negative ionization mode. Other MS conditions were as follows: interface voltage, −3.5 or −3.0 kV; nebulizer N_2 gas, 1.5 or 2.0 liters/min; drying N_2 pressure, 200 or 70 kPa, respectively. Heat block temperature and curved desolvation line temperature were both 200 °C. Analytical conditions were recorded from m/z 250 to 1500 in a negative ionization mode. Atmospheric pressure chemical ionization (APCI) probe temperature was set from 250 to 450 °C.

Analysis of Proanthocyanidin—Proanthocyanidins were characterized by a modified method of Porter *et al.* (11, 12), in which they were degraded to anthocyanidins by heating under acidic conditions. Briefly, 200 μl of purified compound from blueberry leaves (0.1–2.5 mg/ml) was mixed with 750 μl of *n*-butanol/HCl (95:5) and 50 μl of 1% of $NH_4Fe(SO_4)_2 \cdot 12H_2O$ dissolved in 2 M HCl. The mixture was vortexed and heated in an oven at 105 °C for 40 min, and cooled in flowing water. Optical densities of the treated solution were recorded at 540 nm by spectrophotometer (UV-1700, Shimadzu). Procyanidin B2 (Sigma-Aldrich) was used as a standard. The hydrolysates generated by the modified Porter method were also analyzed using LC/MS-IT-TOF as described above. The elution program was 10–40% B linear from 0 to 15 min followed by washing 100% B from 15 to 22.5 min. Electrospray ionization conditions were recorded from m/z 200 to 1500 in a positive ionization mode. Interface voltage and nebulizer N_2 were 4.5 kV and 1.5 L/min, respectively. MS/MS conditions were set to auto system and recorded from m/z 50 to 1000. The parent MS was searched from m/z 200 to 1500, and ion accumulation was 30 ms. The data were analyzed by LCMS solution v3.41 software and Formula Predictor Software (Shimadzu).

Thiolysis Analysis—Thiolysis was performed by a previously described method (13, 14) with some modifications. Briefly, 50 μl of purified samples (2 mg/ml in methanol) was mixed with 50 μl of methanol acidified with HCl (3.3%) and 100 μl of benzyl mercaptan (5% in methanol). The reaction was carried out at 50 °C for 30 min and then kept at ambient temperature for 3 h. Pure catechin or epicatechin solution (1.25 mg/ml in methanol) (Funakoshi, Tokyo, Japan) was also thiolyzed to obtain the epimerization rate to calculate the ratio of catechin and epicatechin in the terminal units. The reaction mixture was diluted 5-fold with methanol and analyzed by reverse-phase HPLC. An Atlantis T3 column (4.6 mm × 150 mm, 3 μm, Waters) was used at 40 °C as described above. UV detection was performed at 280 nm. The gradient program was 15–25% B linear from 0 to 10 min, 25–100% B linear from 10 to 30 min, followed by washing 100% B from 30 to 37.5 min and re-equilibration of the column 37.5 to 45 min under initial gradient conditions. To ascertain the elution pattern of thiolysis media and to estimate unknown peaks, LC/MS-IT-TOF was also employed in a negative ion mode. Flavan-3-ols and their benzylthio adducts obtained by thiolysis media of procyanidin B2 were used as a standard. The mDP was calculated by the formula, mDP = [sum of (benzylthio adducts × n) + sum of (free flavan-3-ol × n)]/[total free flavan-3-ol], in which "n" is DP of detected flavan-3-ol by thiolysis.

Preparation of Proanthocyanidin from Blueberry Leaves—To prepare proanthocyanidin from blueberry leaves, freeze-dried powder (100 g) was extracted with 1.2 liters of acetone for 10 min, and the supernatant was decanted. This procedure was repeated five times to remove the green pigment from the leaves, followed by washing in 1.2 liters of hexane for 30 min. The remaining residues were washed with ethyl acetate. The washed powder of leaves was extracted with 1.2 liters of methanol for 30 min, and the supernatant was filtered. This procedure was repeated four times, and the resulting crude methanol extracts were concentrated by rotary evaporator at 50 °C and lyophilized, finally resulting in ~30 g of solid powder. The crude methanol extract (15 g) was then dissolved in 1.0 liter of 60% methanol and placed on a Sephadex LH-20 column (50 mm × 920 mm, Amersham Biosciences). Fractionation was performed using the following series of solvents: fraction I, 9.0 liters of 60% methanol (retrieved weight: 10.2 g); fraction II, 9.0 liters of 100% methanol (retrieved weight: 3.3 g); fraction III, 9.0 liters of 70% (v/v) acetone (retrieved weight: 1.3 g). The LC/MS-IT-TOF analyses of each fraction indicated that fraction I was primarily composed of quinic acid, chlorogenic acid, and flavonol glycosides such as rutin. Fraction II consisted of proanthocyanidin oligomers from tetramer to decamer as analyzed by thiolysis. Fraction III consisted of proanthocyanidin polymers that were decamers or greater. In each fraction, the eluate was divided into 28 subfractions/liter.

Northern Blot Analysis—Total RNAs from cultured replicon cells were prepared using RNeasy mini kits (Qiagen). RNAs were denatured at 65 °C for 15 min, cooled on ice, and then separated by 1% agarose-formaldehyde gel electrophoresis (2 μg/lane) and transferred to a positively charged nylon membrane (Hybond-N^+, Amersham Biosciences). The membrane was hybridized with a biotinized probe of the neomycin phosphotransferase gene. For detection of the bound probe, membranes were incubated with streptavidin-Alexa Fluor 680 conjugate (Invitrogen), and the bound fluorescence was detected by Odyssey Infrared Imaging System (LI-COR Biosciences). For internal control, β-actin mRNA-specific biotinized antisense RNA probe was used.

Western Blot Analysis—Cultured replicon cells were harvested, and total cellular proteins were extracted with Cel-Lytic-M (Sigma-Aldrich) containing 1% protease inhibitor mixture (Sigma-Aldrich). The samples were separated by SDS-PAGE using 10% gel under reducing conditions. The proteins were transferred electrophoretically to an Immobilon-P membrane (Millipore, Bedford, MA).

The membrane was treated with a blocking buffer for near infrared fluorescent Western blotting (Rockland, Gilbertsville, PA). Primary antibodies used were anti-human hnRNP A2/B1, hnRNP K, hnRNP L, and hnRNP Q and anti-human β-actin antibodies (EF-67, D-6, A-11, 18E4, and I-19, respectively, Santa Cruz Biotechnology, Santa Cruz, CA), anti-human eukaryotic translation initiation factor 3 (eIF3) F, eIF3G eIF3H polyclonal antibodies (Novus Biologicals, Littleton, CO), and

anti-HCV NS-3 polyclonal antibody (10). The labeled proteins were visualized with Alexa Fluor 680 anti-rabbit or anti-mouse IgG (Invitrogen) or IRDye™ 800CW anti-goat IgG (LI-COR Biosciences) and detected by using as Odyssey Infrared Imaging System.

Affinity Purification of Proanthocyanidin-binding Proteins—Purified blueberry leaf-derived proanthocyanidin or catechin was coupled with epoxy-activated Sepharose 6B (Amersham Biosciences) according to the manufacturer's instructions. Approximately 5×10^8 HCV replicon cells were extracted with lysis buffer (50 mM sodium phosphate (pH 7.5), 1% CHAPS, 5 mM EDTA, 150 mM NaCl, and protease inhibitor mixture (Complete™, Roche Diagnostics, Mannheim, Germany)). The total protein extract (90 mg) was added to the coupled Sepharose beads (3 ml) and incubated at 4 °C overnight with gentle rotation. The beads were centrifuged ($500 \times g$) for 1 min, and the pellet was washed six times with the lysis buffer. The absorbed proteins were eluted by incubation in 2% SDS with 50 mM dithiothreitol at 100 °C for 10 min. The eluate was concentrated with an Amicon Ultra-4 Ultracel-5k (Millipore), and the solvent was replaced by the lysis buffer. Protein concentration was determined by the *o*-phthalaldehyde method using bovine serum albumin as the standard.

Fluorescent Two-dimensional DIGE—Fluorescent two-dimensional-DIGE was performed using fluorescent dyes, IC3-OSu and IC5-OSu (Dojindo Molecular Technologies), with a modification of the methods reported elsewhere (15, 16). Briefly, 10 μg of proteins per gel were precipitated using a two-dimensional clean-up kit (Bio-Rad) and then dissolved in 20 μl of sample buffer (10 mM sodium phosphate (pH 8.0), 7 M urea, 2 M thiourea, 3% CHAPS, and 1% Triton X-100). After addition of 400 pmol of IC3-OSu or IC5-OSu, proteins were incubated at 40 °C for 30 min. The labeling reaction was quenched by incubation with 400 μM lysine for 15 min, followed by addition of an equal volume of the sample buffer with 150 mM dithiothreitol, 0.4% Bio-Lyte 3–10 (Bio-Rad Laboratories), and 0.004% bromphenol blue. Two-dimensional gel electrophoresis was performed according to the manufacturer's instructions (Bio-Rad). The mixed samples were applied to ReadyStrip IPG strips (pH 3–10 NL, 7 cm, Bio-Rad) for separation in the first dimension. The second-dimensional separation was performed by SDS-PAGE using an 8% gel. Fluorescence imaging was performed on a Proxpress™ proteomic imaging system (PerkinElmer Life Sciences). IC3-OSu-labeled proteins were detected with 540/25 nm excitation and 590/35 nm emission filters. IC5-OSu-labeled proteins were detected with 625/35 nm excitation and 680/30 nm emission filters. In this study, while proteins from proanthocyanidin- or catechin-coupled Sepharose were labeled with IC5-OSu, a mixture of equal quantities of both samples was labeled with IC3-OSu and used as a reference for quantitation of IC5-OSu-labeled proteins as described (16). The fluorescent images were aligned using SameSpot TT900 S2S (Nonlinear Dynamics, Newcastle, UK) and then analyzed with Progenesis Discovery software (Nonlinear Dynamics). Each group (eluate from proanthocyanidin- or catechin-coupled Sepharose) was run on triplicate gels three times. Spot intensity in the IC5-OSu image was normalized to the intensity of the corresponding IC3-OSu image spot in the same gel. The average spot intensities ± standard deviation (S.D.) from nine gels were calculated. Statistical differences were determined by Student's *t* test, and *p* values <0.05 were considered significant. The proteins having high affinity to proanthocyanidin but not to catechin were detected using a 1.5-fold change ($p < 0.05$) as the cut off.

Protein Identification—Protein identification by peptide mass fingerprinting was performed as described previously (17). Briefly, 100 μg of proteins was separated by two-dimensional-DIGE gels and stained with Coomassie Brilliant Blue R-250. Protein spots of interest were excised from the gel and digested overnight with trypsin. Each peptide extract was deposited onto a thin layer of α-cyano-4-hydroxycinnamic acid (Bruker Daltonics, Bremen, Germany) and allowed to adsorb for 5 min, after which the layers were washed twice with 0.1% trifluoroacetic acid. Spectra were obtained using matrix-assisted laser desorption/ionization-TOF-TOF-MS, Autoflex II TOF/TOF (Bruker Daltonics) in positive-ion and reflectron mode. The data set was entered in an in-house Mascot search engine (Matrix Science, London, UK), to find the closest match with known proteins registered in the data base from the Swiss-Prot.

Knockdown of Proanthocyanidin-binding Proteins Using siRNAs—ON-TARGETplus SMARTpools of duplex siRNAs targeting hnRNP L, hnRNP K, hnRNP A2/B1, hnRNP A/B, hnRNP Q, eIF3F, eIF3G, eIF3H, and non-targeting control siRNA were purchased from Dharmacon (Thermo Fisher Scientific, Tokyo, Japan). Individual sequence of hnRNP A2/B1 siRNAs was confirmed by two single siRNAs (Target #09: 5′-CGGUGGAAAUUUCGGACCA-3′, Target #11: 5′-GGAGAGUAGUUGAGCCAAA-3′). The replicon cells were transfected with each siRNA using Lipofectamine RNAiMAX reagent (Invitrogen) according to the manufacturer's protocol. After 72 h incubation, the cells were assayed.

RESULTS

Purification of an Inhibitor of HCV Subgenome Expression from Blueberry Leaves—We screened 283 species of local agricultural products for their suppressive activity against the expression of subgenomic HCV RNA using an HCV replicon cell system, and found significant suppressive activity in the leaves of the blueberry (*Vaccinium virgatum* Aiton), peels of roots of Taro (*Colocasia esculenta* L.), and hulls of seeds of Japanese plum (*Prunus mume* Sieb. *et* Zucc). Among them, extracts of blueberry leaves contained the highest total activities. Therefore, we purified a compound from blueberry leaves that inhibited expression of subgenomic HCV RNA in replicon cells. An overall purification scheme is shown in Fig. 1, and a summary of the purification steps is shown in Table 1. From 1000 mg of lyophilized powder from the leaves, 440 mg of methanol extracts was obtained. The IC_{50} value of the methanol extracts was 5.47 μg/ml. The inhibitory activity was recovered in the CMW-W fraction (284.2 mg), in which the IC_{50} value was 1.74 μg/ml. The specific activity of CMW-W was 3-fold greater than that of the initial methanol extracts and the yield of the activity exceeded 200%, suggesting that an interfering substance had been removed.

The CMW-W fraction was subjected to a subsequent HPLC purification step in which a preliminary HPLC elution pattern

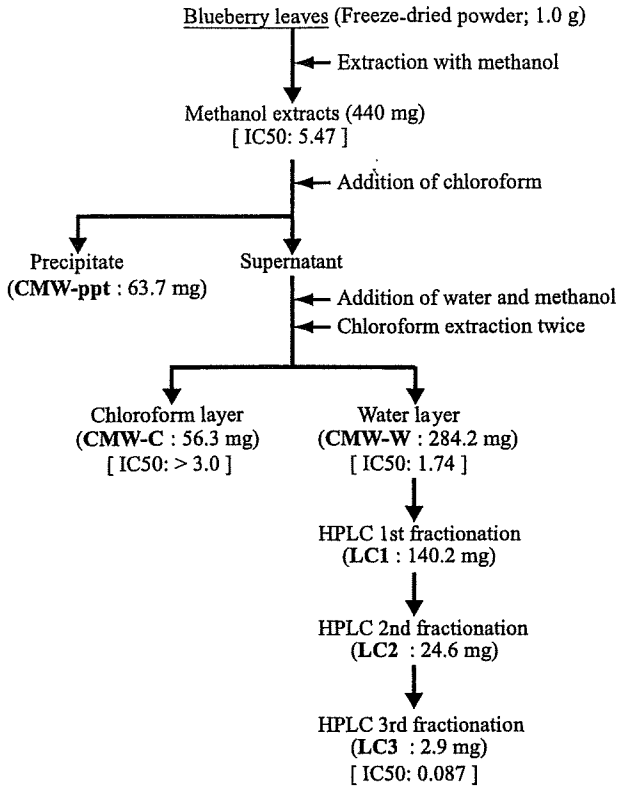

FIGURE 1. **Fractionation of blueberry leaf extract for the inhibitor of HCV subgenome expression.** The inhibitory activity was indicated under each fraction as the IC_{50} value (micrograms/ml).

TABLE 1
Purification of HCV subgenome expression inhibitory activity in blueberry leaf

	Total weight	Subgenome expression, IC_{50}	Specific activity	Purification factor	Total activity	Yield
	mg	*μg/ml*	$1/IC_{50}$		mg/IC_{50}	%
MeOH extract	440.0	5.47	0.18	1.00	80.44	100
Water layer	284.2	1.74	0.57	3.14	163.33	203.05
LC 1st	140.2	0.89	1.12	6.15	157.53	195.84
LC 2nd	24.6	0.54	1.85	10.13	45.56	56.63
LC 3rd	2.9	0.087	11.49	62.87	33.33	41.44

(a 15–100% gradient of acetonitrile) was used. The data indicated that a strong inhibitory activity eluted around 90% of acetonitrile (17 min) with some minor inhibitory activities broadly eluted earlier. Those results suggested the possible existence of multiple HCV subgenome expression inhibitors in the CMW-W fraction (Fig. 2*A*). To purify the most active component, we initially separated the CMW-W isocratic at 30% acetonitrile and collected the active fraction eluted at 3.3–5.2 min (Fig. 2*B*). After repeated collection, we obtained 140.2 mg of active fraction (LC1) from 440 mg of methanol extracts. The IC_{50} value of this fraction for HCV RNA expression was 0.89 μg/ml, yielding a specific activity 6-fold higher than that of the initial methanol extracts (Table 1). In the second round HPLC (Fig. 2*C*), we fractioned LC1 as follows: 20% acetonitrile from 0 to 7.5 min, followed by 20–100% linear gradient of acetonitrile from 7.5 to 12.5 min. A highly active fraction was eluted from 11.9 to 13.2 min and collected (LC2), yielding 24.6 mg with an IC_{50} value 0.54 μg/ml (Table 1). In the third HPLC step (Fig. 2*D*), we applied LC2 and eluted with 40–65% methanol instead of acetonitrile. The active fraction was eluted from 3.2 to 6.2 min and collected (LC3), finally yielding 2.9 mg of solid material with a dark flesh color. The IC_{50} value for HCV RNA expression of LC3 was 0.087 μg/ml, with a 63-fold increase in specific activity relative to the initial methanol extracts (Table 1). We also checked the cytotoxic effect on replicon cells. The CC_{50} value of the cytotoxicity of LC3 was 18.5 μg/ml, and the selective index, which was calculated by dividing CC_{50} by IC_{50}, was 212.6, showing a 16.5-fold higher selective index value compared with initial methanol extracts (Fig. 3).

The Inhibitor of HCV Subgenome Expression Is Proanthocyanidin—To analyze the constituent elements in the purified fraction LC3, EPMA was performed. This analysis indicated that the fraction is composed of carbon and oxygen, but not nitrogen (data not shown). In addition, trace amounts of calcium, sodium, potassium, and aluminum, which appeared to be contaminating elements, were also identified. Next, LC3 was analyzed by LC/MS-IT-TOF. Preliminary trials showed that analysis required the use of an APCI probe at 450 °C, and no signal was obtained at 250 °C. The mass spectrum data showed five peaks (Fig. 4), and $[M-H]^-$ at *m/z* 401.0494 and 689.1135 were considered to be trifluoroacetic acid adducts of *m/z* 287.0553 and 575.1196, respectively. From these spectra, the parent mass of this compound appeared to be $[M-H]^-$ at *m/z* 575.1196, which was estimated to be $C_{30}H_{24}O_{12}$ (error = 0.17 ppm), an A-type dimer of procyanidin. Given the fact that strict conditions (APCI probe temperature at 450 °C) were required to ionize the compound, it appeared that the isolate consisted of one or more polymers of procyanidin.

We next analyzed the purified LC3 fraction by butanol-HCl hydrolysis (Porter method) (11, 12). The reacted solution turned a red color, which is in accordance with the color of anthocyanidin generated by heating of procyanidin/proanthocyanidin under acidic condition. Using procyanidin B2 as a standard, the procyanidin content in the LC3 fraction was 86.33%. The hydrolysis solution was analyzed by LC/MS-IT-TOF. The main peak (retention time = 7.3 min) of the PDA chromatogram at 540 nm was observed at the same position as that of the cyanidin standard (Fig. 5*A*). Indeed, MS/MS spectra of this peak were identical to those of the cyanidin standard (Fig. 5*B*). These results revealed that the HCV RNA replication inhibitory compound present in the LC3 fraction from blueberry leaves was procyanidin. Because the hydrolysate of this compound also contained a trace amount of delphinidin (Fig. 5*A*, *arrow*), this compound was considered to be proanthocyanidin rather than procyanidin.

Structural Analysis of the Inhibitory Proanthocyanidin by Thiolysis—To analyze the terminal and extension units and also define mDP of proanthocyanidin in the purified LC3 fraction of blueberry leaves, we combined thiolysis (13) with reversed-phase HPLC. When thiolysis products of purified proanthocyanidin in the LC3 fraction were analyzed in reversed-phase HPLC, several peaks (*A–H*) were identified (Fig. 6). The peaks *A*, *C*, and *H* were considered to be catechin, epicatechin, and benzylmercaptan, respectively, according to the retention time of each standard preparation. Other peaks were confirmed by analyzing mass spectra. The parent mass of peak E was $[M-H]^-$

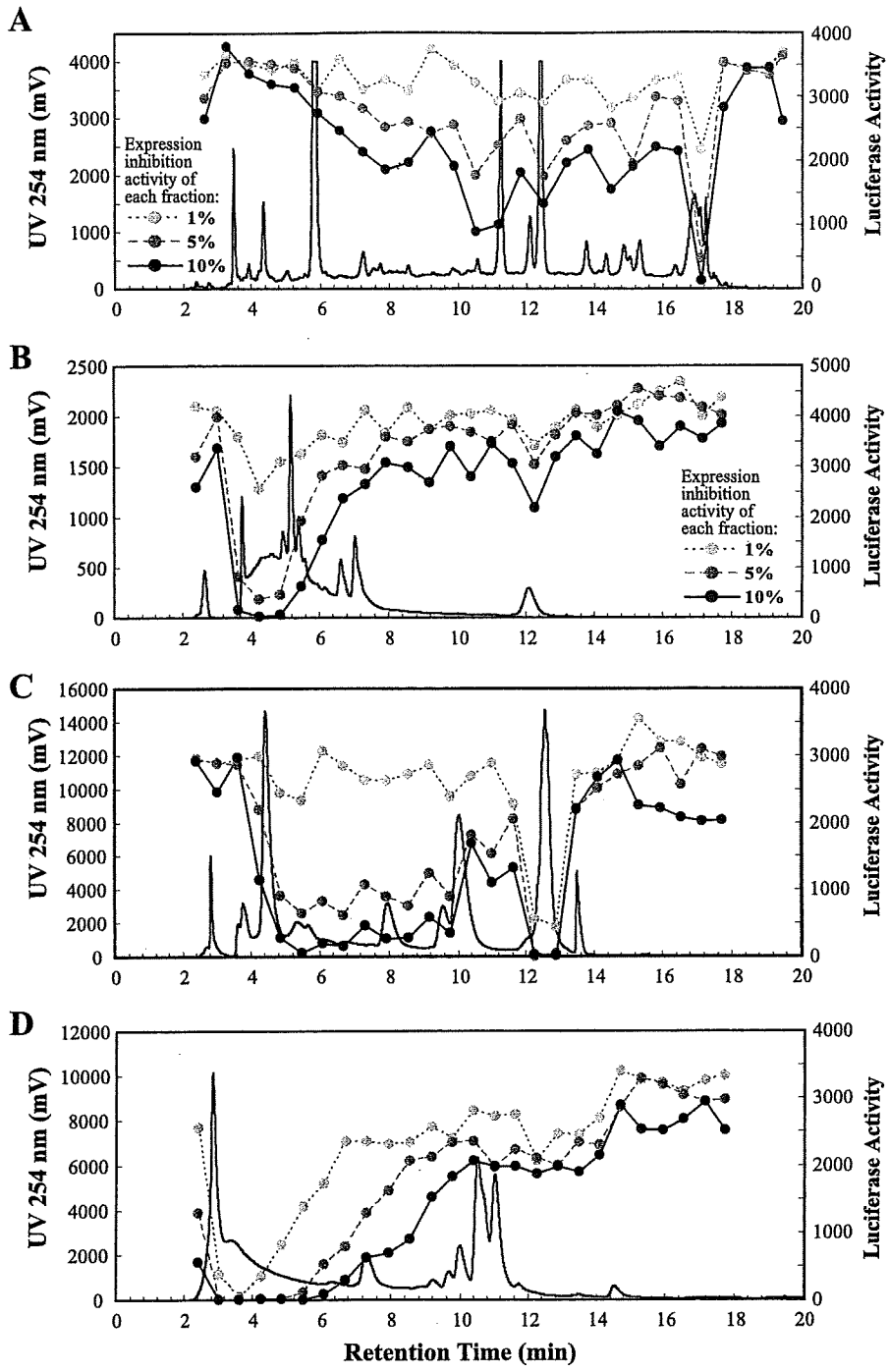

FIGURE 2. **HPLC chromatogram and HCV subgenome expression-inhibitor activity.** Replicon assays were performed using three different concentrations (1%, 5%, and 10%) of each eluted fraction and are indicated as luciferase activity. The elution conditions are indicated under "Experimental Procedures". *A*, preliminary HPLC chromatogram and suppressive activities against HCV subgenome expression in replicon cells. The applied sample was eluted with a 15–100% gradient of acetonitrile. *B*, first preparative fractionation (*LC 1st fractionation*). CMW-W fraction was applied, and the eluate was collected from 2.1 min to 18 min (445 μl/fraction, total 26 fractions). Fractions with significant inhibitory activity, eluted from 3.3 to 5.2 min, were collected. *C*, second preparative fractionation (*LC 2nd fractionation*). The collected sample from the first LC fractionation was subsequently separated by HPLC, and fractions with significant inhibitory activity eluted from 11.9 to 13.2 min were collected. *D*, third preparative fractionation (*LC 3rd fractionation*). Sample collected in the second LC fractionation was further separated by HPLC, and fractions with significant inhibitory activity, eluted from 3.2 to 6.2 min, were collected.

at *m/z* 411.0892, with an estimated formula of $C_{22}H_{20}O_6S$ (error = −3.8 ppm), and its MS/MS spectrum was $[M-H]^-$ at *m/z* 287.0510. The difference between the parental mass and MS/MS was 124.0382, which was in accordance with a benzylthio adduct. Thus, peak E appeared to be catechin or epicatechin benzylthioether. Because the retention time of epicatechin benzylthioether was the same as that of peak E, we considered peak E to be epicatechin benzylthioether. The parental mass of peak G was $[M-H]^-$ at *m/z* 697.1385 (predicted formula: $C_{37}H_{30}O_{12}S$), and its MS/MS was $[M-H]^-$ at *m/z* 573.0987. Again, the difference was 124.0398 and likely represented the benzylthio adduct. Thus, peak G was estimated to be a benzylthioether of A-type dimer consisting of catechin and/or epicatechin. Peak B was detected as parent MS $[M-H]^-$ at *m/z* 863.1822 with a predicted formula $C_{45}H_{36}O_{18}$ (error = −0.86 ppm). Because the formula of B-type procyanidin trimer is $C_{45}H_{38}O_{18}$ and that of A-type is $C_{45}H_{34}O_{18}$, this peak was likely a trimer in which A-type and B-type interflavan bonds coexisted. Peak D was suggested to be an A-B type trimer similar to peak B but with a benzylthio adduct. The parental mass of peak F was $[M-H]^-$ at *m/z* 605.1449, and its MS/MS was $[M-H]^-$ at *m/z* 481.1109, so that a benzylthio adduct was also present in peak F. However, we could not obtain the predicted formula of the parental mass of peak F. The structural analysis of the HCV inhibitor proanthocyanidin from blueberry leaves (fraction LC3) is summarized in Table 2. The mDP of proanthocyanidin in this fraction was estimated to be 7.7. Because the predicted formula of peak F was undefined, peak F is indicated as "unknown" in Table 2.

Role of Polymerized Structure of Proanthocyanidin in the Inhibition of HCV Subgenome Expression—Because the purified HCV expression-inhibitory proanthocyanidin of blueberry leaf was oligomer with mDP 7.7, we asked whether the polymerization was required for inhibitory activity. First, the inhibitory activities of monomers such as catechin, epicatechin, and epigallocatechin-gallate, all of which were constituents of proanthocyanidin, and also of the dimer (procyanidin B2) were

tested by HCV replicon assay. These monomers and the dimer of procyanidin lacked inhibitory activity (Table 3).

We then determined how the degree of polymerization of proanthocyanidin affected the inhibition. The crude fraction of proanthocyanidins was obtained by the extraction of three low polarity solvents (acetone-hexane-ethyl acetate) as described under "Experimental Procedures." The IC_{50} of HCV RNA expression of this proanthocyanidin-enriched fraction was 3.20 μg/ml, showing greater activity than the crude methanol extract. After fractionation on a Sephadex LH-20 column, each eluant was analyzed by LC/MS-IT-TOF and thiolysis to determine the components and mDP of proanthocyanidin (supplemental Fig. S1). Then, the blueberry leaf-derived proanthocyanidins with different mDP were assessed for HCV inhibitory activity. The inhibitory activity of blueberry leaf proanthocyanidin was clearly dependent on the polymerization level, and the peak activity was observed at a polymerization level of ~8 to 9 (IC_{50}: 0.05 μg/ml) (Fig. 7).

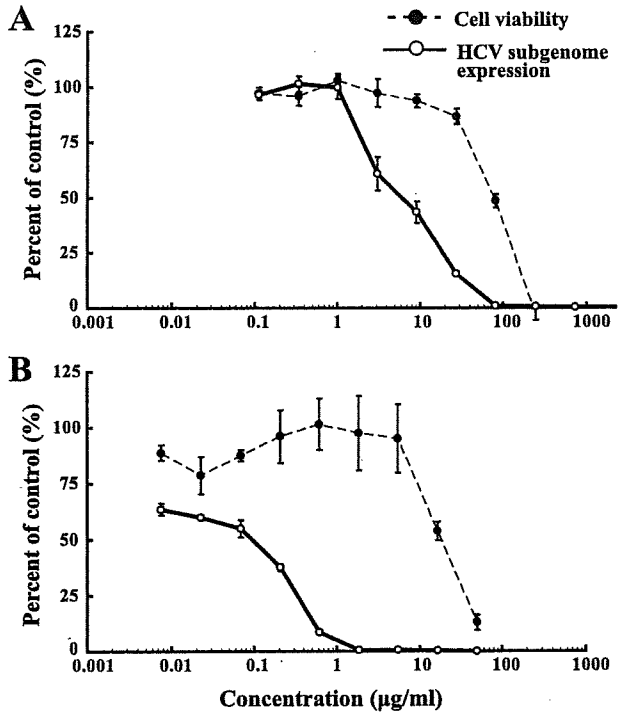

FIGURE 3. **Dose-dependent effects of blueberry-derived samples on subgenomic HCV RNA-expression inhibition and viability of replicon cells.** *A*, dose-dependent effects of methanol extracts of blueberry leaves. Concentrations of the sample from 0.112–2200 μg/ml were tested. IC_{50} for HCV expression and CC_{50} for cytotoxicity were 5.47 μg/ml and 70.61 μg/ml, respectively, and the selective index was 12.9. *B*, dose-dependent effects of purified sample (LC 3rd fractionation). Concentrations of the sample from 0.01 to 50 μg/ml were tested. The IC_{50} values for HCV subgenome expression and cytotoxicity were 0.087 μg/ml and 18.50 μg/ml, respectively, and the selective index was 212.6.

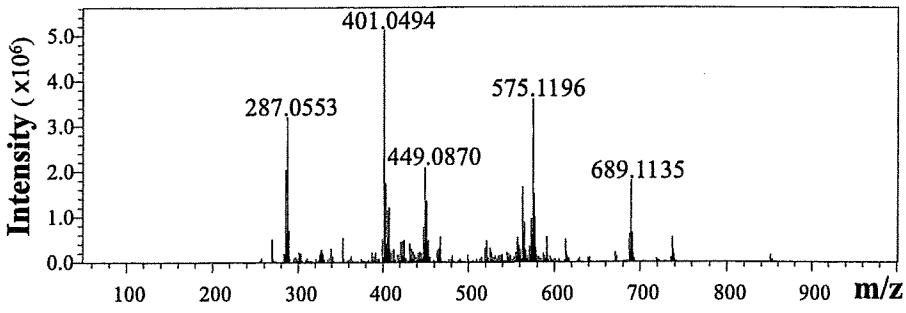

FIGURE 4. **APCI MS spectra of the LC3 fraction.** The total-ion chromatogram of the LC3 fraction was further analyzed by APCI MS. Peaks of *m/z* 401.0494 and *m/z* 689.1135 were considered to be trifluoroacetic acid adducts of *m/z* 287.0553 and *m/z* 575.1196, respectively. Parental MS of this compound was estimated at *m/z* 575.1196, and the formula was assumed to be $C_{30}H_{24}O_{12}$.

Effect of Purified Blueberry Proanthocyanidin on the Expression of NS3 HCV Protein in Replicon Cells—In our system, HCV RNA expression in replicon cells was expressed as luciferase activity. Thus, the observed inhibitory activity may have resulted from nonspecific inhibition of luciferase by proanthocyanidin. Therefore, we examined the effect of the purified proanthocyanidin (fraction LC3) on the expression levels of the neomycin-resistant gene and the NS3 protein gene, both of which were encoded in the HCV subgenome of replicon cells. The purified blueberry proanthocyanidin suppressed the expression of the neomycin-resistant gene and also the levels of NS3 protein in a concentration-dependent manner, indicating that the proanthocyanidin purified from blueberry leaves in fact suppressed the expression of HCV subgenome in the replicon cells (Fig. 8).

hnRNP A2/B1, Which Has Affinity to Proanthocyanidin, Is Indispensable for Expression of Subgenomic HCV RNA—To investigate the molecular mechanism underlying the suppression of HCV RNA expression by proanthocyanidin, we comprehensively identified proteins having affinity to the purified proanthocyanidin from blueberry leaves. The protein extract from replicon cells was treated with proanthocyanidin-coupled Sepharose, and then the adsorbed proteins were eluted. The extract was also treated with Sepharose beads coupled to catechin, a structural unit of proanthocyanidin, but HCV subgenome-expression inhibitory activity was not observed (Table 3). The proteins having higher affinity to proanthocyanidin than catechin were detected with fluorescent two-dimensional-DIGE (Fig. 9). In the eluate from proanthocyanidin-coupled Sepharose, intensities of 32 spots were increased compared with those from catechin-coupled Sepharose. Twenty-seven spots were cut from Coomassie-stained gels and subjected to peptide mass fingerprinting using MS, and we successfully identified proteins derived from 25 spots (Nos. 1 to 25 in Fig. 9*A* and Table 4). Although other possible candidate spots were also suggested in a rectangular portion (Fig. 9*A*), they were not subjected to protein identification due to insufficient separation.

From the list of identified proteins (Table 4), most could be categorized into two groups. The first group consisted of subunits of eukaryotic translation initiation factor 3 (eIF3). They included eIF3A (spot Nos. 1, 5, and 9), eIF3F (No. 10), eIF3G (No. 12), eIF3H (No. 4), and eIF3M (No. 13). Although eIF3A was identified from multiple protein spots (Nos. 1, 5, and 9), this may be due to post-translational modification and protein processing. The second group of proteins consisted of hnRNPs such as hnRNP A/B (No. 19), hnRNP A2/B1

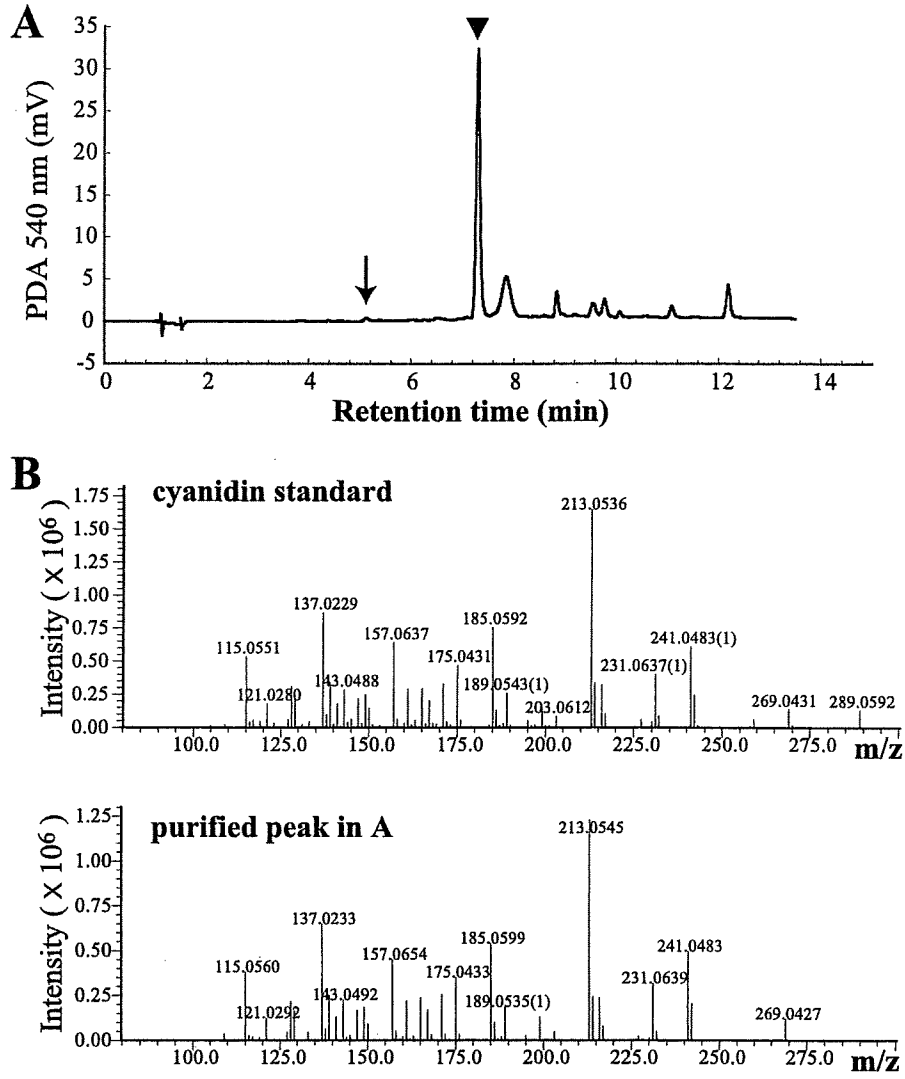

FIGURE 5. **PDA chromatogram and MS/MS spectra of the hydrolysate of the purified fraction by the Porter method.** *A*, PDA chromatogram at 540 nm of hydrolysate of purified fraction from blueberry leaves. The main peak (*arrowhead*; retention time = 7.3 min) is located at the same position as the cyanidin standard. Other peaks were estimated to be methoxylated cyanidins from MS and MS/MS spectra. The *arrow* indicates the position of delphinidin. *B*, MS/MS spectra (positive ion mode) of hydrolysate of cyaniding standard (*upper panel*; parent MS at 287.0550) and the purified peak in A (*lower panel*; parent MS at 287.0555).

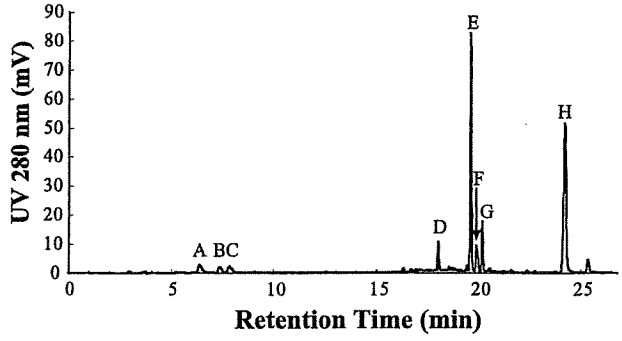

FIGURE 6. **HPLC chromatogram at 280 nm of thiolysis products of LC3 fraction from blueberry leaves.** *Peaks A, C,* and *H* were identified as catechin, epicatechin, and benzylmercaptan, respectively. *Peak E* was identified as epicatechin benzylthioether. *Peaks B* and *D* were estimated to be procyanidin trimer with coexistence of A-type and B-type linkages and its benzylthioether, respectively. *Peak G* was procyanidin A-type dimer. *Peak F* was not identified.

(No. 8), hnRNP K (Nos. 17 and 22), hnRNP L (Nos. 11, 15, and 21), and hnRNP Q (Nos. 2, 6, and 7) also known as NS1-associated protein 1. Importantly, eIF3 has been reported to bind directly to the HCV internal ribosome entry site (IRES), leading to translation initiation of viral proteins (18). Moreover, all hnRNPs identified have been reported to be associated with HCV genomic RNA such as IRES and non-translated regions (19–25). These results imply that proanthocyanidin may target cellular proteins such as eIF3 and hnRNPs. To further clarify the relationship between these proteins and HCV subgenome expression, we examined the effects of siRNA-based knockdown of these proteins (supplemental Fig. S2). First, we selected three eIF3 subunits (eIF3F, eIF3G, and eIF3H), which are thought to be involved in IRES binding of eIF3 (26). However, knockdown of these subunits did not affect the luciferase activity in replicon cells. Then, we targeted all hnRNPs identified. Among them, siRNA pool targeting hnRNP A2/B1 significantly suppressed the luciferase activity of HCV subgenomic replicon cells (supplemental Fig. S2), and this result was confirmed using two kinds of single siRNA (Fig. 10). Weak suppressive activities were also suggested by siRNAs targeting other hnRNPs such as hnRNP A/B, K, and L (supplemental Fig. S2).

DISCUSSION

The HCV infection is a major cause of chronic liver disease, which eventually results in end-stage liver diseases such as cirrhosis and hepatocellular carcinoma. A crude extract from rabbit-eye blueberry (*V. virgatum* Aiton) leaves exhibited significant inhibitory activity against HCV RNA expression when analyzed in HCV subgenomic replicon cells. In this study, we attempted to purify a compound that suppresses HCV subgenome expression from the blueberry leaves. The final purified product was identified as proanthocyanidin, and it was effective at concentrations that are two orders of magnitude below the toxic threshold in replicon cells. The mDP of the proanthocyanidin in purified anti-HCV expression fraction was 7.7 with a high proportion of epicatechin as the monomeric components. Subsequent analysis indicated that the blueberry leaf-derived proanthocyanidin with a degree of polymerization of ~8–9 shows the highest inhibitory activity. Finally, the purified pro-

TABLE 2
Thiolysis results of purified fraction (LC3) from blueberry leaves

	mDP	Terminal				Extension					
		C[a]	EC[b]	AB-3[c]	Total	C[a]	EC[b]	A-2[d]	Unknown	AB-3[c]	Total
		%									
LC3	7.7	20.4	65.1	14.5	100	0.8	58.1	11.9	23.2	6.0	100

[a] Catechin.
[b] Epicatechin.
[c] Trimer consisting of both A-type and B-type interflavan bonds.
[d] A-type dimer.

TABLE 3
Effects of constitutional units of proanthocyanidin on expression of HCV subgenome in replicon cells

Compounds	DP or mDP	Subgenome expression, IC_{50}	Cytotoxicity, CC_{50}	Ratio, CC_{50}/IC_{50}
		μg/ml	*μg/ml*	
Catechin	1	16.18	100.4	6.2
Epicatechin	1	27.32	113.8	4.2
Epigallocatechin-gallate	1	14.61	41.68	2.9
Procyanidin B2[a]	2	>25.0	>25.0	–
Purified proanthocyanidin from blueberry leaf (LC3 fraction)	7.7	0.087	18.5	212.0

[a] Epicatechin dimer.

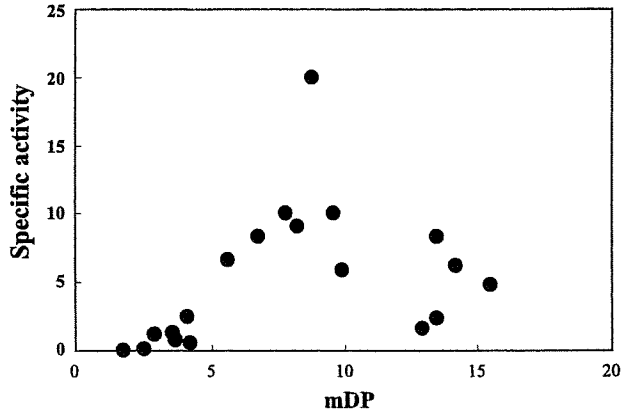

FIGURE 7. **Scatter plot of mDP and specific activity of subgenomic HCV RNA-expression inhibition.** The mDP was estimated by thiolysis of each fraction. The specific activity was calculated from IC_{50} value of each fraction.

anthocyanidin from blueberry leaf extracts suppressed the expression of the neomycin phosphotransferase gene and the NS-3 protein gene in HCV subgenome replicon cells in a dose-dependent manner. These data suggest the potential value of blueberry leaf proanthocyanidin for the treatment of HCV infection.

Proanthocyanidin is a polyphenol that shows polymerization of more than two units of flavan-3-ol such as catechin and epicatechin (supplemental Fig. S3). There are two interflavan bonds in proanthocyanidin, in which the B-type has one linkage of interflavan bond (C4 → C8 or C4 → C6) and the A-type has two linkages of bonds (C4 → C8 and O7 → C2) (27). Proanthocyanidins were previously known as condensed tannin and are present in various plants and foods. They contribute to organoleptic properties such as stability, astringency, and bitterness (28, 29). There are a number of foods and nutritional supplements that contain proanthocyanidins with health-promoting benefits, and their value has been described in the literature and patent documents. For example, proanthocyanidin contained in blueberries increases the lifespan of the nematode (*Caenorhabditis elegans*) (30). Sangre de Grado extracted from *Croton*

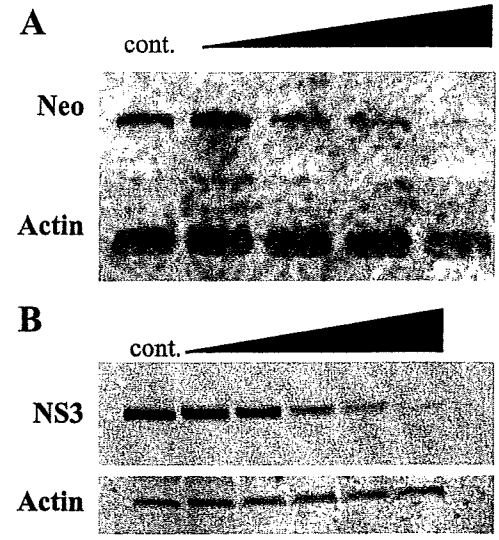

FIGURE 8. **Suppressive effects of purified blueberry leaf proanthocyanidin (LC3 fraction) on the expression of the neomycin resistant gene and NS-3 protein in replicon cells.** *A*, Northern blot analysis of the *neomycin-resistant* gene expression (*Neo*) in the presence of 0 μg/ml (control) to 3.3 μg/ml proanthocyanidin in a 3-fold dilution series. The expression of β-actin mRNA is also indicated as a normalization control. *B*, Western blot analysis of the expression of NS-3 protein (*NS3*) in the presence of 0 μg/ml (control) to 10 μg/ml proanthocyanidin in a 3-fold dilution series. The β-actin protein levels are also shown as a normalization control.

lechleri resin is a traditional natural medicine in the upper Amazon and contains hydrolyzing flavonoids, proanthocyanidins, and other polyphenols (31, 32), which have been shown to possess anti-viral activities against influenza, parainfluenza, herpes simplex viruses, and respiratory syncytial virus (33–38). However, to the best of our knowledge, this report is the first study to demonstrate that proanthocyanidin inhibits the expression of subgenomic HCV RNA.

Regarding the mechanism underlying the anti-viral activities, proanthocyanidins from *Croton lechleri* resin and prodelphinidin B-2 3′-*O*-gallate from green tea leaf inhibit herpes simplex viruses infection by preventing the attachment and penetration of the virus into the target cells (37, 39). Recently, the grapefruit flavonoid naringenin was reported to inhibit apolipoprotein B-dependent HCV secretion (40). However, in this study, we evaluated the inhibitory effect on HCV subgenome expression by measuring luciferase activity in replicon cells without using actual viral particles. Therefore, the mode of anti-HCV action of proanthocyanidin is different from that in herpes simplex viruses infection mentioned above and is also different from the inhibitory mechanism of naringenin. Instead, our study suggests that blueberry leaf-derived proanthocyanidin may interact with hnRNP A2/B1, a factor required for HCV subgenome expression in our replicon assay. In accordance with this observation, recent study has shown that hnRNP A1, a protein highly homologous to hnRNP A2/B1, facilitates HCV replication, and the double knockdown of hnRNP A1 and hnRNP A2 significantly suppresses replication (23). Alternatively, proanthocyanidin may bind to the translational initiation complex associated with HCV IRES and thereby suppresses the HCV subgenome expression, because a number of translational regulatory proteins are included in our list of proanthocyanidin-binding proteins. To date, for the